University of Alberta
Department of Civil Engineering

Structural Engineering Report No. 187

SHEAR LAG IN BOLTED SINGLE AND DOUBLE ANGLE TENSION MEMBERS

by

Yue Wu

and

Geoffrey L. Kulak

June 1993

SHEAR LAG IN BOLTED SINGLE AND DOUBLE ANGLE TENSION MEMBERS

YUE WU

and

GEOFFREY L. KULAK

Structural Engineering Report No. 187

Department of Civil Engineering
The University of Alberta
Edmonton, Alberta, Canada T6G 2G7

June 1993

Acknowledgements

The authors wish to express their thanks to Dr. A.E. Elwi and Dr. D.W. Murray, both of the Department of Civil Engineering, University of Alberta, for their help with the finite element analyses described in this report. Larry Burden and Richard Helfrich, technicians in the Morrison Structural Engineering Laboratory, were of great assistance with the experimental portion of the work.

Dr. Murty K.S. Madugula of the Department of Civil Engineering at the University of Windsor supplied experimental data from several sources that would not otherwise have been available to the authors. This generous sharing of information is greatly appreciated.

Table of Contents

List of Symbols

A_{cn} = net area of connected leg
A_{ne} = effective net area of tension member
A_g = gross area
A_n = net area
A_o = gross area of outstanding leg
d = diameter of fastener hole
E = modulus of elasticity
F_u = ultimate tensile strength
F_y = yield strength
g = gauge, transverse spacing of fastener lines
K_1 = ductility factor
K_2 = fabrication factor
K_3 = geometry factor
K_4 = shear lag factor
L = connection length
L_c = width of connected leg
L_o = width of outstanding leg
n = number of fasteners per line in the direction of applied load
P_u = net section strength of tension member
Q = percent reduction in the area of a standard test coupon (51 mm gauge length)
r = ratio of A_{cn} to A_o
R = distance from end of angle to boundary of gusset plate
s = pitch, distance between two successive holes in the direction of fastener lines
T_r = factored resistance of tension member
U = net section efficiency; reduction coefficient
$\bar{x}$ = eccentricity, distance frome the face of gusset plate to the center of gravity of angle
β = factor to account for the effect of connection length
$\emptyset$ = resistance factor

1. Introduction

1.1 Strength of Angles as Tension Members

Steel angles are widely used in civil engineering structures as axially loaded tension or compression members. For example, they are frequently used in light trusses for both the chord and web members or are used to form the lattice framework in transmission towers. Although different configurations are possible, the most widely used arrangements are as single angles or as a pair of angles symmetrically placed about a gusset plate that passes between them. Both of these arrangements are discussed in this report, and that described for the pair of angles will simply be referred to by the standard terminology, "double angles".

The capacity of axially loaded angles that are loaded in compression is almost always controlled by their local and overall buckling strength. On the other hand, angles that are loaded in axial tension will have a capacity which reflects both the cross-sectional area of the components and the way in which the angles are connected at their ends. For practical reasons, it is unusual to be able to connect both legs, and the influence of the connection of only one of the two legs upon the capacity of the angles is referred to as "shear lag". It is principally this effect of the method of the end connection of angles loaded in tension that is the object of the investigation reported herein. The investigation is limited to the case in which end connections are made using mechanical fasteners. Thus, both the effect of the reduced cross-section resulting from the presence of holes (the "net cross-section") and shear lag will be present in the members under examination. Although several failure modes are possible (e.g., block shear, bearing), only the net section failure mode is investigated in this study.

It is customary to evaluate the capacity of an angle in terms of the ratio of its average stress at ultimate load to the ultimate tensile strength of the material. When mechanical fasteners are used, this ratio is called the net section efficiency (U). Thus, for the case under examination, the net section efficiency is:

$$U = \frac{P_u/A_n}{F_u} \qquad [1.1]$$

where P_u = ultimate capacity of the member

A_n = net cross-sectional area

F_u = ultimate tensile strength of the material

1.2 Statement of the Problem

Most design standards used for fabricated steel tension members base their rules on work done by Munse and Chesson [1, 2]. This work included examination of the capacity of tension members of many different cross-sections, and angles were not particularly set out as a distinctive case. However, there are special attributes associated with single or double angle tension members that suggest that they should not necessarily be included in the general case.

As has already been introduced, in the cases of single angles and double angles it is customary to connect only one leg of each angle. As a result, the axial force in the main region of the member, which presumably acts through the center of gravity of the cross-section, is eccentric with respect to the connected end. Both biaxial bending and the shear lag effect will be present. Tension members which use a symmetrical cross-section, for example, an I-shape, will not have bending present, even though shear lag effects will exist in the usual case wherein only the flanges are used to make the connections at the ends. Finally, although the principal North American standards apparently use the Munse and Chesson studies as the basis for their rules, it will be seen that the specifics differ in some important respects. For example, some standards consider the effect of connection length upon capacity and differentiate between the case of short angle legs connected or long angle legs connected, but others do not. Thus, it is considered appropriate to examine the problem of axially loaded single and double angle tension members as a separate case on its own.

1.3 Objectives

The objectives of this study were to:

1. Conduct physical tests of single and double angle tension members in order to obtain their net section strength and to examine the shear lag effects for a series of parameters;
2. Compare the capacities of single angle members versus double angle members;
3. Examine the current specifications and propose a more rational design approach, if appropriate;
4. Evaluate the stress distribution at the critical cross-section by finite element analysis, and develop finite element models for load versus deflection analysis which can be used in future studies to obtain the capacity of single angles and double angles analytically;
5. Outline areas of future study.

2. Literature Review

2.1 Previous Studies

In 1906 and 1907, McKibben tested 60 tension members made of an angle or a pair of angles [3, 4] to obtain their ultimate strength. Considering only specimens where lug angles[1] were not used, there were 18 single angle specimens and six double angle specimens. The end connections were made using rivets. The net section efficiencies obtained in these tests ranged from 75 to 83 percent, with a mean of 80 percent, for the single angle specimens, and from 77 to 84 percent, with a mean of 81 percent, for the double angle specimens.

Batho investigated the behavior within the elastic range of single angle and double angle members which were connected by rivets [5]. He observed that the double angles did not act as a unit, but each angle bent about its own neutral axis. Strain measurements showed that plane sections remained plane under loading. There was little difference between cases where the load was applied in line with the rivets and cases in which the load was in line with the projection of the centroid of the cross-section on the connected leg. The in-plane stiffness of the gusset plate affected the stress distribution in the member.

Davis and Boomsliter carried out an investigation of welded end connection and riveted end connection tension members that were composed of one or more angles [6]. Among the specimens there were two welded end connection and two riveted end connection single angles and one welded and one riveted end connection double angles. The strains measured at the mid-length cross-section indicated that, within the elastic range, the strain distribution was nonuniform for all single angle specimens and the riveted double angle specimen, but nearly uniform for the welded double angle specimen. The net section efficiencies obtained were 87 percent for the welded double angles and 77 percent for the riveted double angles. For the single angle specimens, the test efficiencies were 70 percent, and there was little difference between the welded and riveted connections.

Based on the test results of McKibben [3, 4] and Greiner [7], Young [8] proposed that the net section efficiency for a single angle member be calculated as:

---

[1] A lug angle is a short length of angle used only in the connection region of angle tension members to assist in transmitting load from the gusset plate to the main member. Thus, the main angle is connected to the gusset plate directly by the connected leg, while the other leg (the so-called outstanding leg) is connected to one leg of the lug angle which has the other leg connected to the gusset plate. It is a detail that is not much used today.

$$U = 1.0 - 0.18 \frac{L_o}{L_c} \qquad [2.1]$$

where L_o is the width of the outstanding (unconnected) leg and L_c is the width of the connected leg.

Single and double angle members with different patterns of welded connections were investigated by Gibson and Wake [9]. They found that there was little difference in the ultimate strengths between balanced and unbalanced arrangements of the welds. (In a balanced welded connection, the welds are arranged so that their working strength capacities are balanced about the projection of the centroid of angle on the connected leg.) It was observed that in the direction perpendicular to the gusset plate, the single angle and the gusset plate were bent in the connection region, and that the shorter the connection, the more severe was the bend. It was also observed that the yielding of the outstanding leg of the double angles extended farther back into the connection region than was the case for the single angle. For the specimens that failed through the cross-section of the angle, the average ultimate strength of double angles was nine percent higher than for otherwise comparable single angles.

Nelson conducted an experiment using 18 single angles connected at their ends by fitted bolts [10]. The effects of member length and the in-plane restraint for the gusset plate were studied. No significant difference was found by doubling the member length or by changing the connection between the gusset plate and the testing machine from a fixed to a pinned connection. From the strain measurement at the critical section, it was noted that the plane of the outstanding leg remained plane during loading and that the compressive yield strain was reached at the edge of the outstanding leg for some specimens. The net section efficiencies obtained in these tests ranged from 64 to 84 percent, with a mean of 75 percent. Nelson found that the efficiency is a function of the number of connection bolts per line as well as the ratio of outstanding leg area to connected leg net area. He proposed an empirical equation based on the test results to calculate the net section efficiency as follows:

$$U = \frac{1}{1 + \frac{r}{n}} \qquad [2.2]$$

where n = number of bolts per line

$r = \frac{A_o}{A_{cn}}$

A_o = gross cross-sectional area of outstanding leg

A_{cn} = net cross-sectional area of connected leg

Hebrant and Demol [11] found that the average efficiency for members with drilled holes is about 14 percent higher than that for members with punched holes. This conclusion was obtained from the test results of single angle members, double angle members, single channel members and double channel members. They also reported that the efficiencies were the same no matter whether the member consisted of a single component or a pair of components. For the angle members particularly, the efficiency was 85 percent for the case of single angles with punched holes, 95 percent for the case of single angles with drilled holes, 86 percent for double angles with punched holes, and 96 percent for double angles with drilled holes.

Munse and Chesson studied a wide range of truss-type tension members using both test results obtained from their own experiments and from others. The specimens studied included different cross-sectional configurations, connections, materials, and fabrication methods. An empirical equation to calculate the net section efficiency was proposed. It was based on the test results of 218 specimens [1], among which there were 56 single angles and 33 double angles (without using lug angles). This equation was verified further by a comparison with more than 1000 test data [2].

Munse and Chesson found that the net section efficiency of tension members with bolted or riveted end connections is a function of a relatively large number of factors. Their conclusions can be expressed using the concept of effective net area [12] as:

$$A_{ne} = K_1 K_2 K_3 K_4 A_n \qquad [2.3]$$

where A_{ne} = effective net area of cross-section

A_n = net area of cross-section

$K_1 = 0.82 + 0.0032\ Q \leq 1$ (Q is described following)

K_2 = 0.85 for members with punched holes

= 1.0 for members with drilled holes

$K_3 = 1.6 - 0.7 \frac{A_n}{A_g}$

A_g = gross area of cross-section

$K_4 = 1 - \frac{\bar{x}}{L}$ ($\bar{x}$ and L are described following)

The factor K_1 is an attempt to account for the ductility of material. The term Q used in the definition of K_1 is the percent reduction in the area of a standard tensile test coupon (51 mm gauge length). The fabrication factor, K_2, is used to account for the reduction in

efficiency due to the effect of punching the holes. To account for the effect of hole spacing on the connection, or the g/d ratio, a geometry factor, K_3, is included. Finally, K_4 is the shear lag factor, which takes into account both the eccentricity in the connected parts and the connection length. In the expression for K_4, $\bar{x}$ refers to the distance from the face of the gusset plate to the center of gravity of the member and L is the connection length, taken as the distance between extreme fasteners. Using the test results of more than 1000 tension members of different types, Munse and Chesson noted that Eq. 2.3 predicted the net section efficiency within a ± 10 percent range for most of the test data.

In 1988, Madugula and Mohan [13] summarized the design approaches for computing the ultimate strength of bolted single angles in accordance with the following five specifications: the American Association of State Highway and Transportation Officials (AASHTO) [14], the American Institute of Steel Construction (AISC) [15, 16], the Canadian Standards Association (CSA) [17], and the British Standards Institute [18]. These specifications were compared with the test results of Nelson [10], Mueller and Wagner [19], and an experimental program carried out for Western American Power Administration in the United States [20]. Madugula and Mohan observed that certain combinations of edge distance, end distance, and pitch may cause the block shear mode of failure instead of net section failure. Although there was no specific design equation proposed, they concluded that a distinction should be made when predicting the ultimate strengths of angles connected by the long leg or by the short leg.

2.2 Current Design Specifications

To compute the net section strength of tension members in a way that includes the shear lag effect, an "effective" net area is used instead of the net area in order to take into account the reduction of efficiency as a result of this effect. Generally, the effective net area is defined as :

$$A_{ne} = U\, A_n \qquad [2.4]$$

where U is the net section efficiency (also called reduction coefficient). The net cross-sectional area (A_n) is to be computed according to the $s^2/4g$ rule [21] if the fastener holes are staggered.

Both AASHTO [22] and American Railway Engineering Association (AREA) [23] treat the design of angles in the same way. For the single angle connected by one leg, the effective net area is taken as the net area of connected leg plus one-half of the area of

outstanding leg. For a double angle member in which each angle has one leg connected and one not connected, the net area is considered to be fully effective. In all cases, when computing the net area, the hole diameter is taken 2 mm (1/16 in.) larger than the actual size in order to account for the effect of punched holes.

For both single and double angles with bolted or riveted connections, the AISC codes [16, 24] and CAN/CSA-S16.1-M89 [21] use a reduction coefficient (U) to compute the effective net area by Eq. 2.4. To calculate the net area (A_n), the hole width is to be taken as 2 mm (1/16 in.) greater than the nominal dimension of the hole according to the AISC codes, but this allowance may be waived in CAN/CSA-S16.1-M89 if the hole is known to be drilled rather than punched. The reduction coefficient U is 0.85 for connections with no fewer than three fasteners per line in the direction of stress and 0.75 for the connections with only two fasteners per line. The derivation of these coefficients will be discussed in detail in Chapter 6.

In the American Society of Civil Engineers (ASCE) standard [25], the allowable tensile stress on concentrically loaded tension members is the yield stress (F_y). For angles used as tension members, the allowable tensile stress on the net area of plain and lipped angles connected by one leg is $0.9F_y$. If the legs are unequal and the short leg is connected, the unconnected leg shall be considered to be the same size as the connected leg.

Obviously, there is inconsistency among these specifications. For example, double angle members are considered 100 percent effective by AASHTO and AREA, while AISC and CSA assign the same reduction coefficient for double angles as for a single angle. The effect of connection length is not included at all in the specifications of AASHTO, AREA, and ASCE. For an angle with unequal leg sizes, it is to be expected that there will be some difference in strengths between the cases with the long leg connected and the short leg connected; however, the AISC specifications and CAN/CSA-S16.1-M89 prescribe the same strength for these cases.

3. Experimental Program

3.1 General

The purpose of the experimental program was to examine the shear lag effect upon the net section strength of single and double angle tension members. The parameters that were considered likely to have an effect on shear lag comprise the following:

1. Length of the member;
2. Length of the connection;
3. Size and disposition of the cross-section, including angle thickness and whether the long leg or the short leg is connected;
4. For the case of single angles, the out-of-plane stiffness of the gusset plate.

In addition to the examination of net section strength of the angles, the stress distribution at selected cross-sections and the deformations of specimens under loading were also investigated.

The total number of specimens was twenty-four, and these encompassed twenty individual configurations of specimens. Only bolted end connections were used and only one line of bolts was considered. The failure mode of block shear was excluded when the specimens were designed.

3.2 Coupons

In order to establish basic material properties, two tension coupons were taken from near the mid-length of each of 14 source angles that were used to make up the 24 full-size test specimens. One coupon was taken from the extremity of each leg. The dimensions of the coupons were in accordance with the requirements of American Society for Testing and Materials (ASTM) [26]; a gauge length of 200 mm was used and coupon widths were 25 mm for the 51 mm wide angle legs and 38 mm for the 76 mm and the 102 mm wide legs.

An extensometer with a 25 mm gauge length was used to measure the strain in the coupon and the load was obtained as a read-out of the testing machine. Pairs of strain gauges were mounted on both faces of four coupons in order to verify the extensometer measurement. Elongation over the coupon gauge length at rupture was measured after failure.

3.3 Specimen Description

The specimens were prepared from fourteen individual pieces of angle, which was to meet the requirements of CAN/CSA G40.21-M 300W [27]. Each of the fourteen pieces

was about 6100 mm long. The two individual angles of what was to be a double angle specimen were always taken from the same stock angle. Cross-section properties were measured at three locations along the length of a specimen; the average values are reported in Table 3.1.

Specimen designation and description are presented in Table 3.2, which should be used in conjunction with Fig. 3.1. Single angle specimens are designated S and double angle specimens are designated D. Each of the eleven single angle specimens tested has some feature that distinguishes it from any of the others; hence, the number in the single angle designation is simply sequential. The double angle specimens are also listed simply in a sequential fashion. However, there is some duplication within this group, and so a second number is used to identify this feature. For example, the designation D3-2 identifies the third double angle member tested in sequence and the second of the set within that group. The out-of-plane stiffness of the gusset plate for single angle members is represented by the distance from the start of the angle to the fixed boundary and is shown as the dimension "R" in Fig. 3.1.

Specimens were designed so that failure would occur at the net section. Standard gauges were used and the bolting details followed the requirements of CAN/CSA-S16.1-M89 [21]. The slenderness ratio satisfied the requirement of that standard for both single angle and double angle specimens, and in all cases there was no resultant need for intermittent fillers for the double angles.

All holes were punched to a diameter of 24 mm and these accommodated 22 mm dia. A490 bolts in a bearing-type connection. Gusset plates were prepared from steel meeting CAN/CSA G40.21-M Grade 300W. The gusset plates for double angle specimens were reused for an entire phase of the test set-ups, while those for single angle specimens were used only once because bending of the plate took place in each test.

3.4 Test Setup

The experimental program was done in two phases. Specimens D1-1, D1-2, D1-3, D3-1 and D4-1 were tested in the first phase while all the others were done in the second phase. The distinction between the two phases is simply that slightly different end fixture conditions were used.

In most practical cases, gusset plates are fixed at one boundary and no in-plane rotation is allowed at that location. The test setups were designed to model this boundary condition. When the test program started, a set of clevises was used to transmit the loads from the testing machine to the specimens (termed, first phase). The gusset plates were pin-connected to the clevises, as shown schematically in Fig. 3.2. These were all double

angle specimens and, because of the symmetry of the double angles, there was no lateral movement perpendicular to the gusset plate. Shims were inserted between the gusset plates and the clevises to prevent any in-plane rotation of the gusset plates. A dial gauge was installed to measure potential in-plane movement at the top of the lower gusset plate. Thus, any tendency for in-plane rotation of the gusset plate could be observed during the test.

After the first five tests described above had been done, it was decided to use a different arrangement to transmit the load from the testing machine to the test specimens. This test setup, termed second phase, is shown in Fig. 3.3. Now the load was applied to the specimens through hydraulic grips that gripped the gusset plates at the two ends. The pressure of the grips was chosen in such a way that the in-plane rotation of the gusset plates was restrained completely, but such that the gripped material would not yield under this pressure. For single angle specimens, the out-of-plane movement of the gusset plates was also fixed at the gripped areas in this arrangement because the hydraulic grips could be locked into place after alignment was completed.

The instrumentation used is shown in Fig. 3.4 for the single angle tests and in Fig. 3.5 for the double angle tests. Electrical resistance strain gauges were mounted at both the mid-length section of the member and in the connection region. In the latter case, the gauges were at the two critical sections at the last bolts of the top and bottom connections. For double angle specimens in the first phase, strain gauges were arranged symmetrically for both angles, but in the second phase only one of the two angles was monitored. In order to measure the bending curvature of single angle specimens in the direction perpendicular to the gusset plate, two gauges were mounted on the opposite sides of the connected leg at the location 25 mm away from the top gusset plate. All gauges were oriented to measure the strains in the longitudinal direction.

The elongations of a specimen were measured separately on the connected leg and on the outstanding leg by linear variable differential transformers (LVDT's). The total elongation, which included the elongation of the angle and the gusset plates, the deformation of the bolts, and the slip of the connections, if any, was measured by both the stroke of the testing machine and by a cable transducer attached to the crosshead of the machine.

As shown in Fig. 3.4 and Fig. 3.5, lateral deflections were measured in the directions parallel and perpendicular to the gusset plate by means of LVDT's in the first phase and cable transducers in the second phase. In the direction parallel to the gusset plate, five locations were monitored for both single angle and double angle specimens. In the perpendicular direction, five locations were monitored for a single angle, while only the mid-length point was measured for a double angle specimen.

Whitewash was applied throughout a specimen so that visual identification could be made of yielding regions.

3.5 Test Procedure

The top and bottom gusset plates were first installed in either the clevises or the hydraulic grips. After alignment was considered to be satisfactory, the specimen was connected to the gusset plates by bolts, which were lightly tightened but not yet at the so-called "snug-tight" condition. About ten percent of the expected yield load of the specimen was then applied to seat the specimen such that the bolts were bearing against the gusset plate and the angle. In this way, major slip of the connections during the loading was unlikely. While the load was being held, the bolts were turned to the "snug-tight" condition by a wrench, and then tightened additionally to provide the required bolt tension. In the first phase tests, a spud wrench was used for the additional tightening, which was one-third turn past the snug-tight condition. In the second phase tests, an impact wrench was used to pre-tension the bolts to one-third turn past snug. After all the bolts had been tightened to the desired condition, the axial load in the angles was released and the specimen was returned to the condition of zero axial load.

All instrumentation was read under zero load and then the stroke of the testing machine was used to apply deformation to the test specimen. At regular intervals, the stroke was held constant such that the specimen was allowed to redistribute the stress and static load readings were obtained. Readings of strain gauges, LVDT's and cable transducers were taken continually during the loading process. An x-y plotter was used to monitor the load versus elongation behavior of the test.

Table 3.1 Measured Properties of Cross-Sections

Specimen	Thickness (mm)	Leg Dimensions (mm)		Area (mm^2)	
		Connected Leg	Unconnected Leg	Gross	Net[1]
S1	6.52	102	102	1288	1122
S2	6.49	102	102	1281	1116
S3	6.54	102	101	1287	1120
S4	4.90	76.1	74.8	716	591
S5	6.44	103	73.8	1099	936
S6	6.41	74.5	103	1100	937
S7	6.43	103	74.6	1100	937
S8	9.61	75.9	50.8	1126	882
S9	4.76	76.9	50.5	584	463
S10	4.70	77.3	50.4	578	459
S11	4.72	77.0	50.5	580	460
D1-1	6.51	102	102	2570	2239
D1-2	6.51	102	102	2568	2237
D1-3	6.52	102	101	2564	2233
D2	4.92	76.3	74.8	1438	1188
D3-1	6.46	103	73.9	2203	1875
D3-2	6.43	103	74.4	2205	1878
D4-1	6.47	74.2	103	2209	1880
D4-2	6.42	74.6	103	2198	1872
D5	6.42	103	74.5	2203	1876
D6	9.53	75.8	50.8	2231	1747
D7	4.71	76.7	50.5	1154	915
D8	4.71	77.2	50.6	1160	920
D9	4.70	77.1	50.6	1157	918

Note: 1. The net areas are computed using a hole width 2 mm larger than the actual size.

Table 3.2 Specimen Description (See also Fig. 3.1)

Specimen	Size (mm)	Connected Leg (mm)	No. of Bolts, n	Member Length, L (mm)	Bolt Gauge, g (mm)	R (mm)
S1	102x102x6.4	102	6	2036	63.5	50.8
S2	102x102x6.4	102	6	2036	63.5	101.6
S3	102x102x6.4	102	6	2036	63.5	152.4
S4	76x76x4.8	76	6	2036	44.5	50.8
S5	102x76x6.4	102	6	2096	63.5	50.8
S6	102x76x6.4	76	6	2096	44.5	50.8
S7	102x76x6.4	102	6	2776	63.5	50.8
S8	76x51x9.5	76	6	1976	44.5	50.8
S9	76x51x4.8	76	6	1976	44.5	50.8
S10	76x51x4.8	76	4	1992	44.5	50.8
S11	76x51x4.8	76	2	1992	44.5	50.8
D1-1	102x102x6.4	102	6	1786	63.5	N.A.[1]
D1-2	102x102x6.4	102	6	1786	63.5	N.A.
D1-3	102x102x6.4	102	6	1786	63.5	N.A.
D2	76x76x4.8	76	6	1786	44.5	N.A.
D3-1	102x76x6.4	102	6	1786	63.5	N.A.
D3-2	102x76x6.4	102	6	1786	63.5	N.A.
D4-1	102x76x6.4	76	6	1786	44.5	N.A.
D4-2	102x76x6.4	76	6	1786	44.5	N.A.
D5	102x76x6.4	102	6	2776	63.5	N.A.
D6	76x51x9.5	76	6	1786	44.5	N.A.
D7	76x51x4.8	76	6	1786	44.5	N.A.
D8	76x51x4.8	76	4	1792	44.5	N.A.
D9	76x51x4.8	76	2	1792	44.5	N.A.

Note: 1. R is not applied to double angle specimens since the out-of-plane stiffness of the gusset plate for double angle specimens has no effect on the behavior of these specimens.

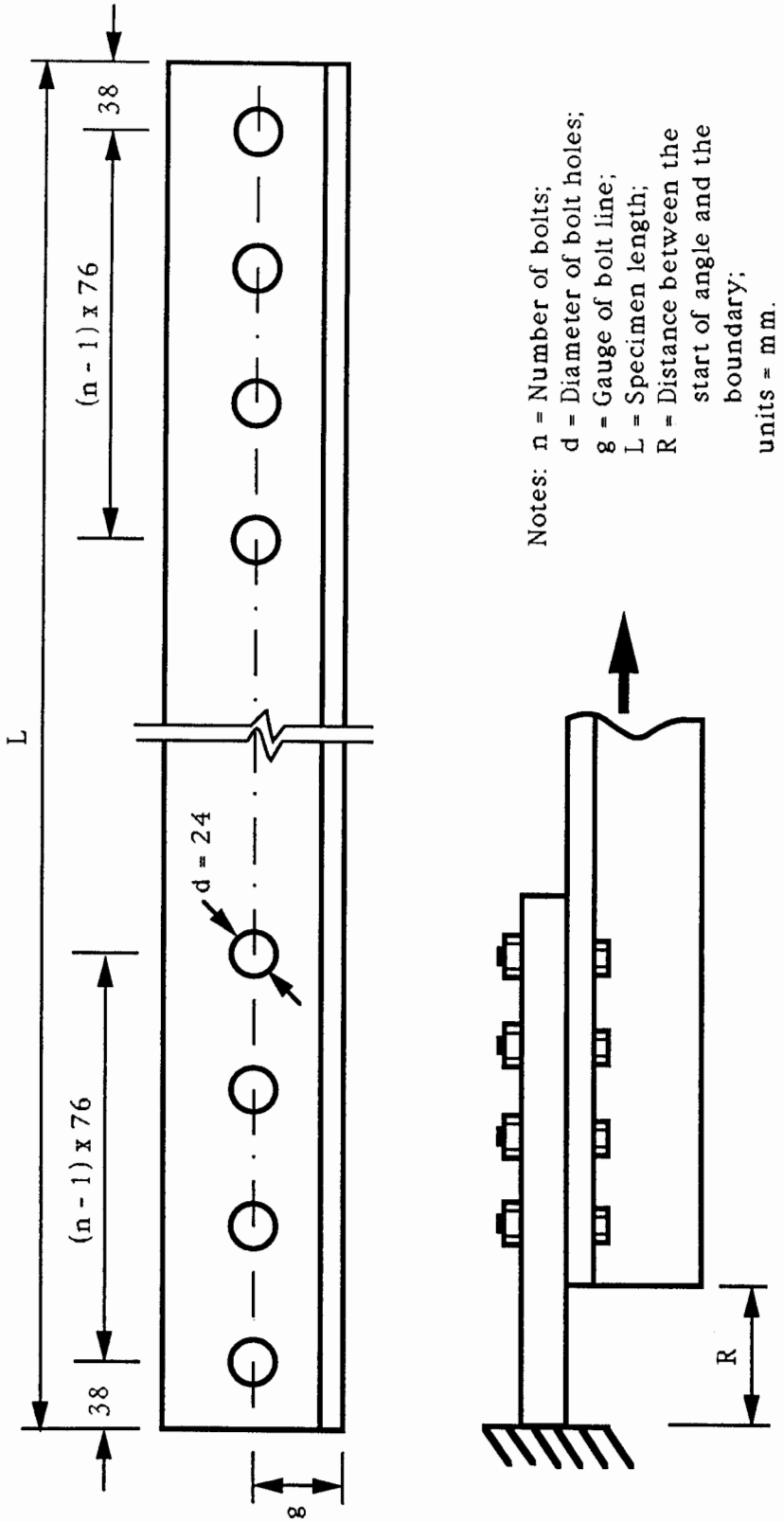

Figure 3.1 Specimen Dimensions

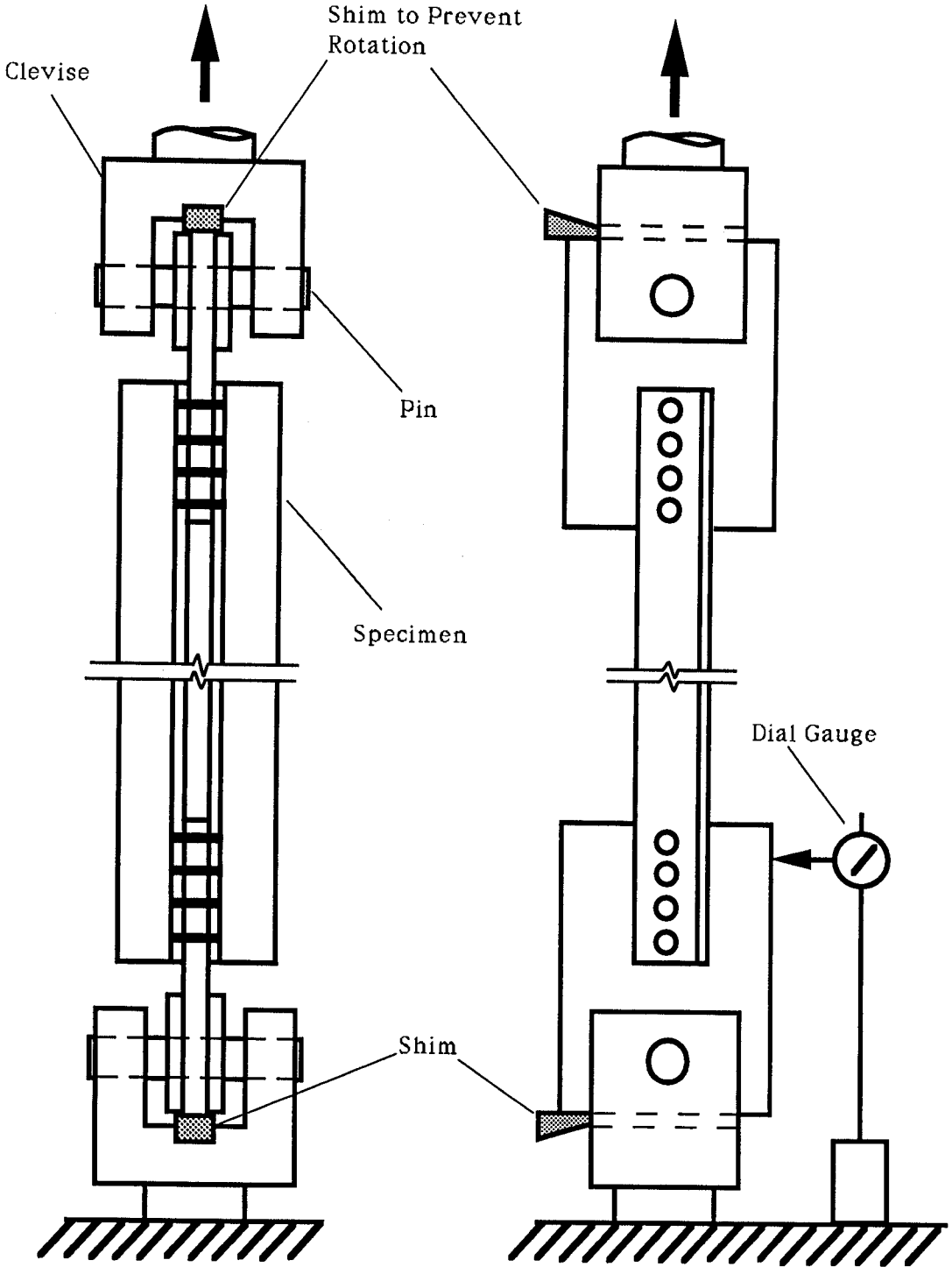

Figure 3.2 Test Setup - First Phase

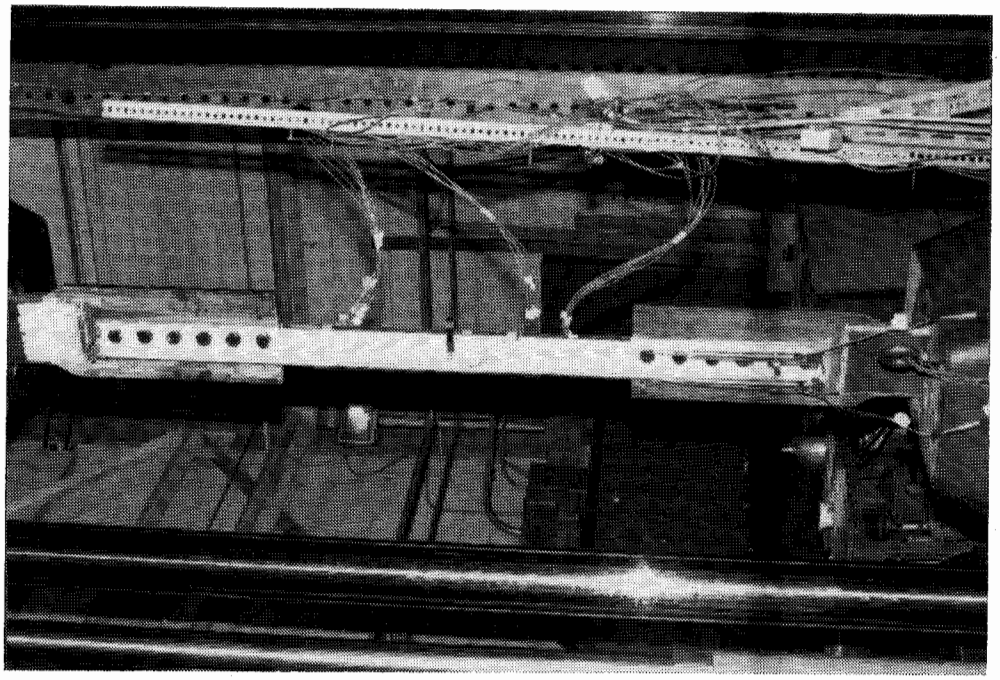

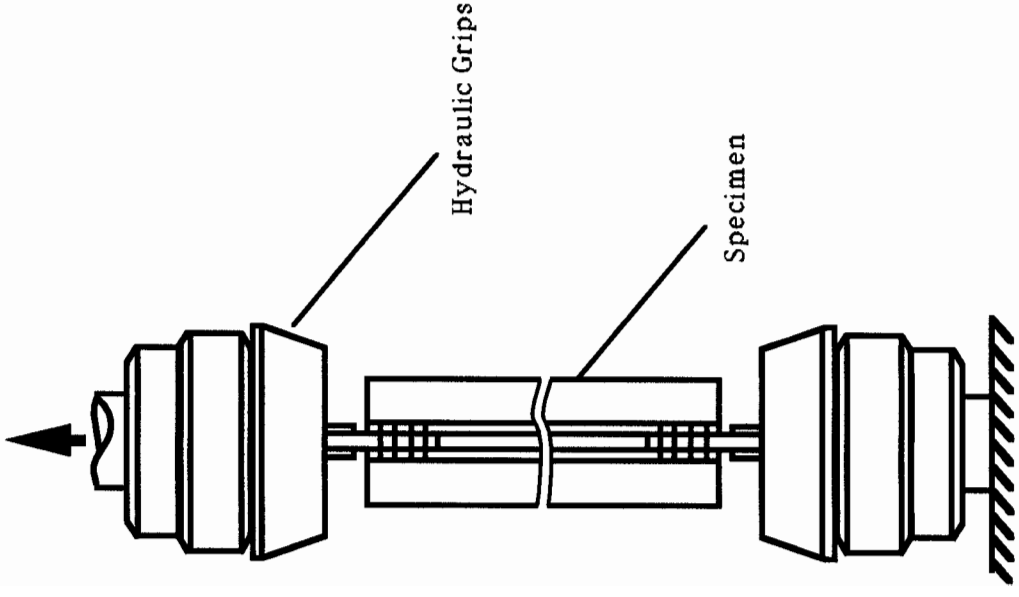

Figure 3.3 Test Setup - Second Phase

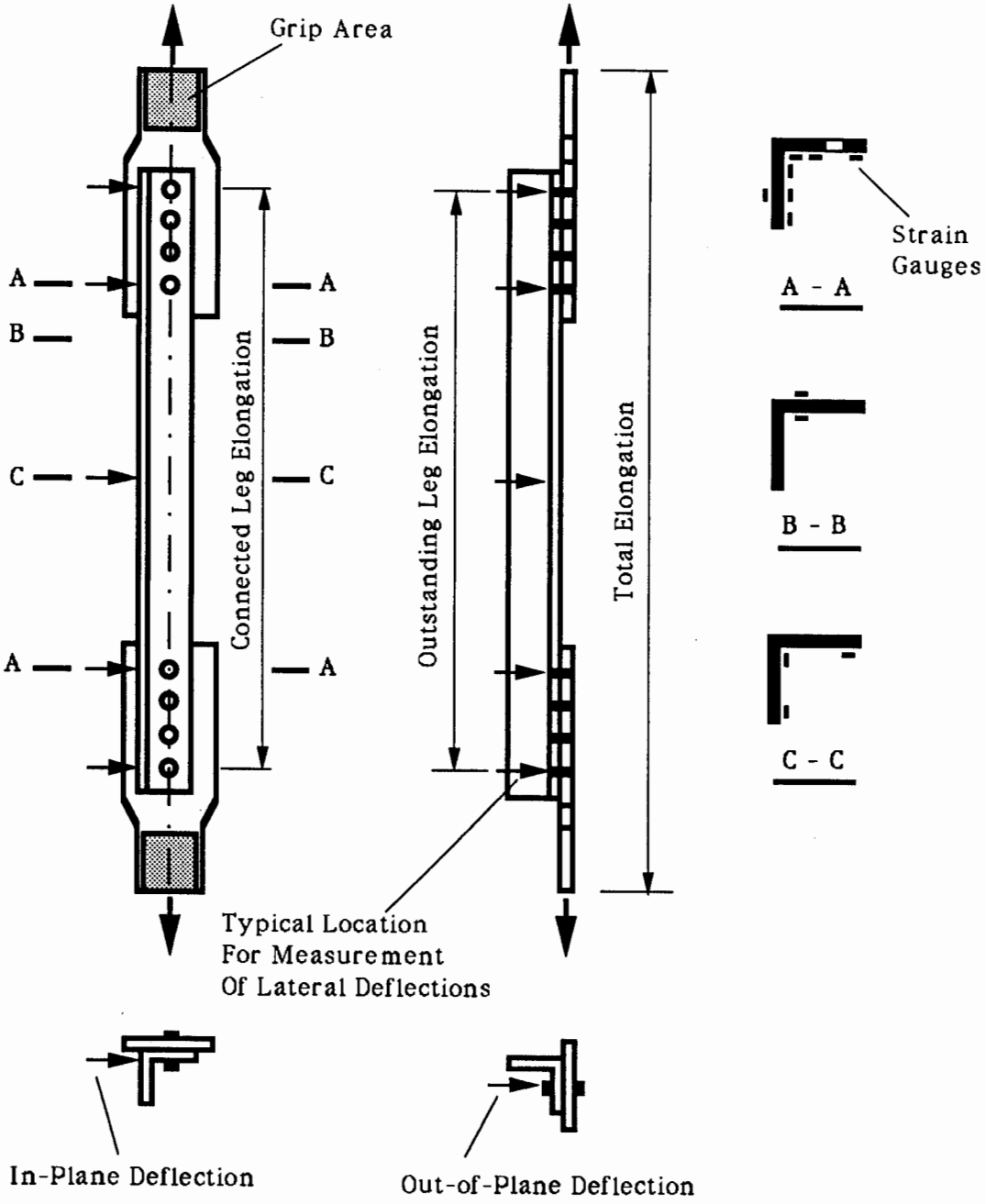

Figure 3.4 Instrumentation of Single Angles

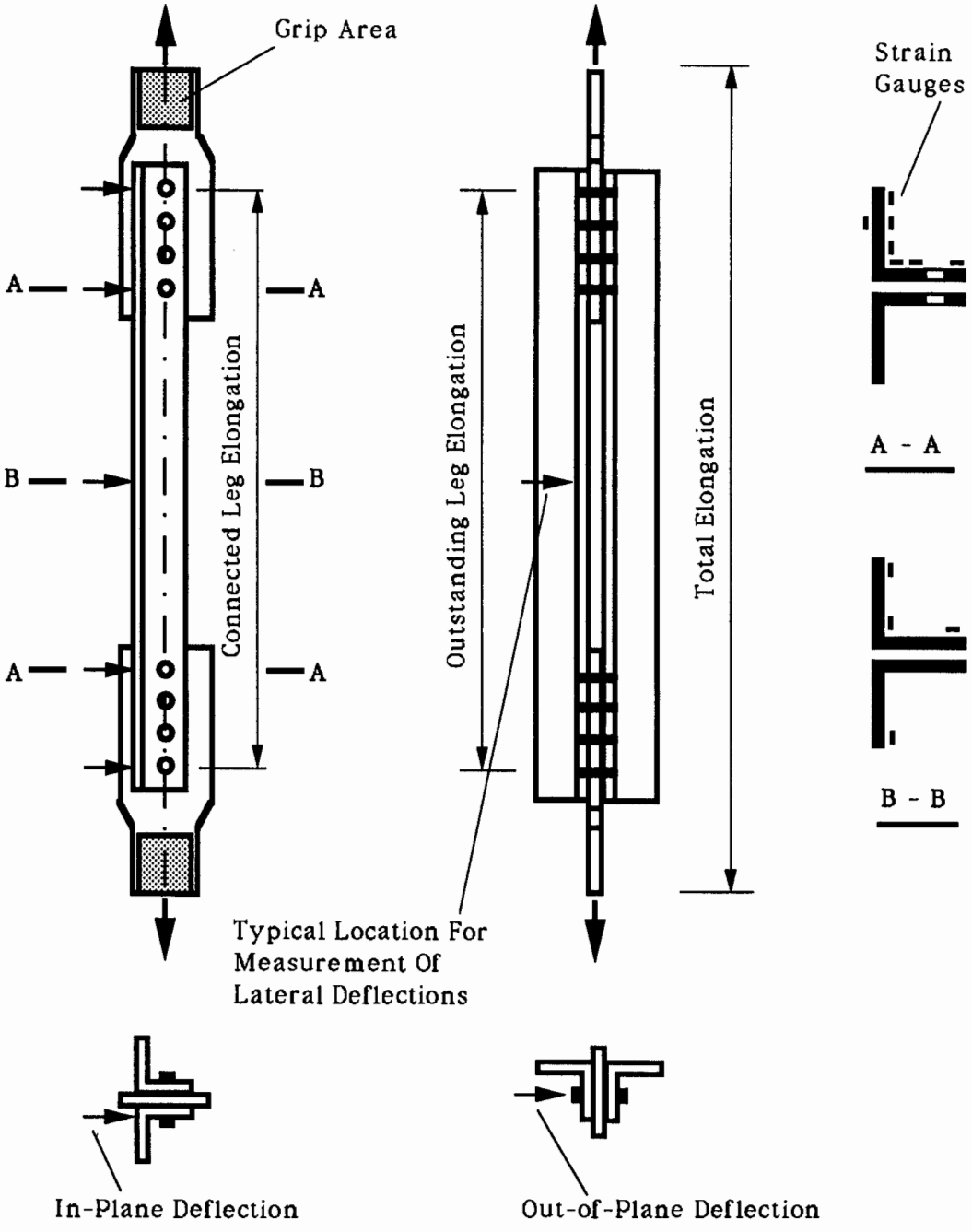

Figure 3.5 Instrumentation of Double Angles

4. Test Results

4.1 Coupon Tests

The material properties of the tensile coupons taken from the angle stock are presented in Table 4.1. The values reported for each specimen are the average values of the two coupons taken from the piece of angle which was later used to make the specimen indicated. The average modulus of elasticity for all specimens was 202 100 MPa. The average static yield strength, static ultimate strength, and dynamic ultimate strength were 331 MPa, 490 MPa, and 525 MPa, respectively. The average strain at the ultimate strength was 18 percent and the average elongation of the coupon gauge length at rupture was 25 percent.

It was found that the extensometer readings taken on the four coupons where strain gauges were also mounted were essentially the same as the corresponding strain gauge readings, within the valid reading range.

4.2 Full Scale Test Results

4.2.1 General Observations and Ultimate Strength

From the readings of the dial gauge which was used in the first phase to measure the in-plane rotation of the gusset plate (Fig. 3.2), it was found that the maximum value of this rotation was only about one degree. Comparison of the test results between the first phase and the second phase (where there was no in-plane rotation at all) for the two pairs of identical specimens, D3-1 with D3-2 and D4-1 with D4-2, showed that there was little difference between these two tests in which the conditions of end restraint were nominally different.

As load was applied, the first yield lines started at the critical sections of the angles, around the bolts. As the load increased, the yielded region extended out from the critical sections to the mid-length of the angle on both the connected leg and the outstanding leg. By the time the load reached its ultimate value, basically the whole region between the two critical sections was yielded, as can be seen in Fig. 4.1 and 4.2, except the cases of specimens S11, D7 and D9, where only a portion of the specimens close to the critical sections was found to be yielded. In the cases of specimens S11 and D9, a compression yielded zone was found at the outstanding leg of the critical section.

During the loading process, the gusset plates of double angle members remained straight. However, in the case of the single angles the gusset plate and the angle bent during the loading. This kind of bending, referred as global bending, can be seen in Fig. 4.3. As the load was being applied, the corners of the angle at the two ends gradually

separated from the gusset plates for both single and double angle members. Thus, a gap was formed between the corner of the connected leg and the gusset plate (termed local bending), as can also be seen in Fig. 4.3. The visible length of the gap was usually from the start of the angle to the second bolt, or sometimes the third bolt. Because the bolts had been pretensioned, the corner of the angle was actually bending about the bolt line. The width of the gap varied from one specimen to another, with a maximum observed value of 10 mm. Generally, the larger gaps were associated with those cases of greater eccentricity of the cross-section, larger gauge of the bolts, smaller angle thicknesses, and shorter connection lengths.

There was no major slip of the connections observed except in the case of specimen D3-2. All the specimens failed at the critical cross-section as the ultimate load was reached. After necking, the critical section was torn out from the edge of the connected leg to the hole, then to the corner of the angle, and eventually the whole angle was broken. The specimen could carry some amount of load beyond the ultimate load and until the whole section was broken. It was noted that all the bolts were still tight after completion of the tests.

The strain gauge readings on the two angles of the double angle specimens in the first phase reflected the symmetry, as expected. Also, the strain gauge readings and the measurement of the lateral deflections were basically symmetrical about the mid-length for all the specimens.

The ultimate strength of the specimens is listed in Table 4.2, where the dynamic (slowly applied) ultimate load is reported. The efficiency of the member is calculated using the dynamic ultimate load and the measured dynamic ultimate strength of the coupon material.

4.2.2 Deformations

The deformation behavior of the test specimens is reported in this section. The elongation, which reflects the ductility of a member, is discussed first, and the elongation reported herein is the total elongation measured by the cable transducer which ran between the crosshead of the testing machine and its base. Next, out-of-plane deflection perpendicular to the gusset plate is discussed. Finally, the in-plane deflection parallel to the gusset plate is reported.

The load versus elongation curves of specimens S1, S2 and S3 are plotted in Fig. 4.4 to illustrate the effect of the out-of-plane stiffness of the gusset plate. Since the width and thickness of gusset plates were identical for all single angle members, the out-of-plane stiffness of the plate is reflected directly in the dimension R, tabulated in Table 3.2, which

is the distance from the fixed end of the gusset plate to the start of the angles. It can be seen that the strength and the ductility of specimen S3, which had the least stiff gusset plate, was a little lower than the others. However, differences in behavior between S1, S2, and S3 were small.

The effect of different connection lengths can be seen in the load versus elongation curves of Fig. 4.5. Specimens S9, S10, and S11 were all single angle specimens of size 76 x 51 x 4.8, which used six, four, and two bolts, respectively, in the end connection. As expected, the specimen with the shortest connection (S11) had the lowest ultimate strength and the ductility was poor. The ultimate strengths for the long connection (S9) and the intermediate length connection (S10) were close to each other, but the ductility of S10 was about 50 percent higher than that of S9. This phenomenon can be attributed to the distribution of shear forces among bolts [28]. The shear force distribution among the bolts of a long joint is much more uneven than it is in a short joint. Consequently, the shear force in the last bolt of specimen S9 could be enough greater than that in specimen S10 such that a more severe local deformation might occur in the critical section of specimen S9, thereby reducing the ductility.

The behavior of a long specimen (S7) and a short specimen (S5) is shown in Fig. 4.6. Each of these specimens (102 x 76 x 6.4 single angles) was identical in all respects except for member length: Specimen S5 was 2096 mm long and S7 was 2776 mm long. The elongations are approximately proportional to their lengths.

There was a clear difference in behavior between specimens with the same cross-section but different dispositions, i.e., long leg connected versus short leg connected. Fig. 4.7 presents the behavior of two specimens that are identical (102 x 76 x 6.4 single angles) except that the long leg is connected in one case (S5), while the short leg is connected in the other (S6). The ductility for the specimen with long leg connected was about twice that for the same cross-section with short leg connected.

Although the cases discussed above are only the single angle specimens, the double angle specimens showed about the same trends in ductility behavior as did the single angles.

In the direction perpendicular to the gusset plate, the out-of-plane lateral deflection at the mid-length of the double angles was very small and could be ignored. As expected, the single angle was flexible in the same direction, however. The deflected shape of some single angle specimens can be seen in Fig. 4.1. Under loading, the single angle tended to deform such that at the mid-length the center of gravity of the angle coincided with the line of action of the applied load. The out-of-plane lateral deflections of specimens S5 and S6 are plotted as a function of the load in Fig. 4.8. For these specimens, which are identical

(102 x 76 x 6.4 single angles) except that the long leg is connected in one case (S5), while the short leg is connected in the other (S6), the mid-length deflection at the ultimate load was 18.5 mm for S5 and 30 mm for S6. These values correspond to 99 percent and 95 percent, respectively, of the eccentricities in that direction, in which eccentricity is the distance from the centroid of the cross-section to the face of the gusset plate. In fact, all of the single angle specimens with six bolt connections had out-of-plane lateral deflections at mid-length equal or close to their eccentricities in the same direction. For those specimens with four bolts or two bolts connections, for example, S10 and S11, the deflections were 75 percent and 53 percent of the eccentricities, respectively. The results for six, four, and two bolt connections (S9, S10, and S11) are plotted in Fig. 4.9. This indicates that the short connection limited the deformation of the angle such that the stresses were not allowed to redistribute as well as in the longer connections.

In the other direction, parallel to the gusset plate, the in-plane lateral deflection of the single and double angle members was small as compared with the out-of-plane deflection of the single angle members. The in-plane deflection for both single angles and double angles reached only 19 percent of the in-plane eccentricity on average. (In-plane eccentricity is the distance from the bolt line to the centroid of the cross-section measured in the direction parallel to the gusset plate.) A typical load versus deflection curve is plotted in Fig. 4.10, and the in-plane deflected shape of some double angles can be seen in Fig. 4.2.

4.2.3 Strain Distribution

Fig. 4.11 shows the load versus strain curves at the critical section of specimen S1 (102 x 102 x 6.4 angle, six bolt connection). As expected, the strain was largest at the edge of the connected leg and smallest at the edge of the outstanding leg. The edge of the outstanding leg was in compression under loads up to about 90 percent of the ultimate load; after that it was in tension. The strain at the edge of the outstanding leg was just around the tensile yield strain at the ultimate load. For angles with short connections, the edge of the outstanding leg was in compression throughout. As shown in Fig. 4.12, the strain measured at the edge of the outstanding leg of S11 (76 x 51 x 4.8 angle, two bolt connection) reached a value close to the compressive yield strain. The load versus strain curves for the mid-length section of S3 (102 x 102 x 6.4 angle, six bolt connection) are shown in Fig. 4.13. At low loads, the strain distribution was nonuniform and the edge of the outstanding leg was in compression. As the load increased, that compressive strain shifted to tension and increased quickly. Eventually, the strains of the whole section were about uniform as the centroid of the angle coincided with the applied load.

Because of the stress concentration around the bolt holes, the strains measured on the

critical section of the connected leg usually had wide variations for both single and double angles. However, the strain distribution on the critical section of the outstanding leg showed some regular patterns, where it was observed that there were basically two types of strain distribution patterns. These can be seen in Fig. 4.14, where the strain distributions of S6 and D4-2 are shown for different levels of load. These two specimens are the same (102 x 76 x 6.4 angles, short leg connected, and six bolt connections) except that S6 is a single angle and D4-2 is a double angle member. The strain distribution of S6 was linear during the entire loading history, whereas the strain distribution of D4-2 changed from nonlinear to linear as the load increased.

It was found that the linear strain distribution pattern described for S6 was typical for all single angle members. This linear strain distribution throughout the loading process reflects the bending deformation perpendicular to the gusset plate, which was described in Section 4.2.1 as in terms of global bending and local bending.

Some double angle members had the strain distribution pattern that has been described for D4-2 (Fig. 4.14), but others had a strain distribution pattern that was similar to that of the single angle members. The inconsistency of the strain distribution among double angle members is probably a reflection of the amount of so-called local bending that is present. For the double angle members that are associated with relatively large amounts of local bending, the strain distribution was linear from beginning to end. Specimen D9 is a typical example of a double angle specimen that has linear strain distribution throughout. The connection length of D9 was short (two bolt connection), so that the local bending extended from the end of the angle to the critical section. In this way, the bending deformation at the critical section was large enough to cause the linear strain distribution at the beginning of loading. On the other hand, if the local bending is limited by a long length connection or by the small gauge of bolt line, bending is unlikely to occur on the critical section when the load is small. Thus, the load is transferred from the connected leg to the outstanding leg mainly by shear deformation (shear lag). The shear deformation produces the nonlinear strain distribution, as shown for D4-2 in Fig. 4.14. After the local bending has developed to a certain degree as the load increases, the critical section has bending deformation, and the strain distribution becomes linear.

The extent of bending of the outstanding leg (perpendicular to the gusset plate) can be measured by the curvature. As shown in the insertion of Fig. 4.15, the curvature is defined as the angle change of the critical section of the outstanding leg. To calculate the curvature at each load level, the strain distribution at the critical section is obtained by a linear curve fit of the measured strains.

Although some double angles had a linear strain distribution throughout the loading

history, as did as single angles, it was observed that the curvature of all double angle members was much smaller than that of the comparable single angles. For example, S2 and D1-2 are identical in all respects (102 x 102 x 6.4 angle, six bolt connection) except that S6 is a single angle member while D1-2 has two angles. As shown in Fig. 4.15, the curvature of D1-2 is only about ten percent of the curvature of S2 at the ultimate load. The difference between the curvatures indicates that single angle members have much larger bending deformation than do the comparable double angle members. This is in agreement with the observation in the experiment, in which a single angle showed both global bending and local bending, while double angles only had local bending.

Table 4.1 Material Properties

Specimen	Modulus of Elasticity (MPa)	Static Yield Strength (MPa)	Static Ultimate Strength (MPa)	Dynamic Ultimate Strength (MPa)	Strain at Ultimate (%)	Elongation at Rupture (%)
S1 & D1-1	200 140	339.8	523.9	562.6	17.7	24.2
S2 & D1-2	197 910	336.6	527.4	564.4	17.0	24.0
S3 & D1-3	199 180	333.3	523.8	560.6	16.7	23.2
S4 & D2	201 515	321.9	472.8	506.5	18.8	26.6
S5 & D3-1	207 580	326.8	481.4	515.4	18.4	25.4
S6 & D3-2	207 710	323.9	477.1	511.7	18.0	25.0
D4-1	202 790	327.4	481.4	515.5	18.4	24.7
D4-2	199 690	323.8	476.8	510.9	17.5	26.0
D5	200 880	325.4	475.8	510.6	17.5	24.6
S7	198 370	324.8	477.7	510.9	18.3	24.2
S8 & D6	204 625	333.4	488.0	521.3	17.0	24.6
S9 & D	203 280	340.4	487.8	523.1	16.6	23.1
S10 & D8	201 120	339.9	485.4	520.6	17.7	25.3
S11 & D9	204 850	338.8	487.2	522.7	17.6	25.2

Table 4.2 Ultimate Load and Efficiency

Specimen	Size (mm)	No. of Bolts per Line	Ultimate Load (kN)	Efficiency[1] (%)
S1	102 x 102 x 6.4	6	512.8	81.2
S2	102 x 102 x 6.4	6	520.8	82.7
S3	102 x 102 x 6.4	6	487.1	77.6
S4	76 x 76 x 4.8	6	276.9	92.5
S5	102 x 76 x 6.4	6	446.4	92.5
S6	102 x 76 x 6.4	6	404.9	84.5
S7	102 x 76 x 6.4	6	432.9	90.4
S8	76 x 51 x 9.5	6	415.2	90.3
S9	76 x 51 x 4.8	6	233.5	96.4
S10	76 x 51 x 4.8	4	239.6	100
S11	76 x 51 x 4.8	2	198.4	82.5
D1-1	102 x 102 x 6.4	6	973.3	77.3
D1-2	102 x 102 x 6.4	6	997.2	79.0
D1-3	102 x 102 x 6.4	6	990.0	79.1
D2	76 x 76 x 4.8	6	492.3	81.8
D3-1	102 x 76 x 6.4	6	838.0	86.7
D3-2	102 x 76 x 6.4	6	850.2	88.5
D4-1	102 x 76 x 6.4	6	797.3	82.3
D4-2	102 x 76 x 6.4	6	782.1	81.8
D5	102 x 76 x 6.4	6	857.2	89.5
D6	76 x 51 x 9.5	6	814.8	89.5
D7	76 x 51 x 4.8	6	412.8	86.3
D8	76 x 51 x 4.8	4	429.4	89.7
D9	76 x 51 x 4.8	2	344.6	71.8

Note: 1. Efficiency (U) $= \dfrac{P_u/A_n}{F_u}$

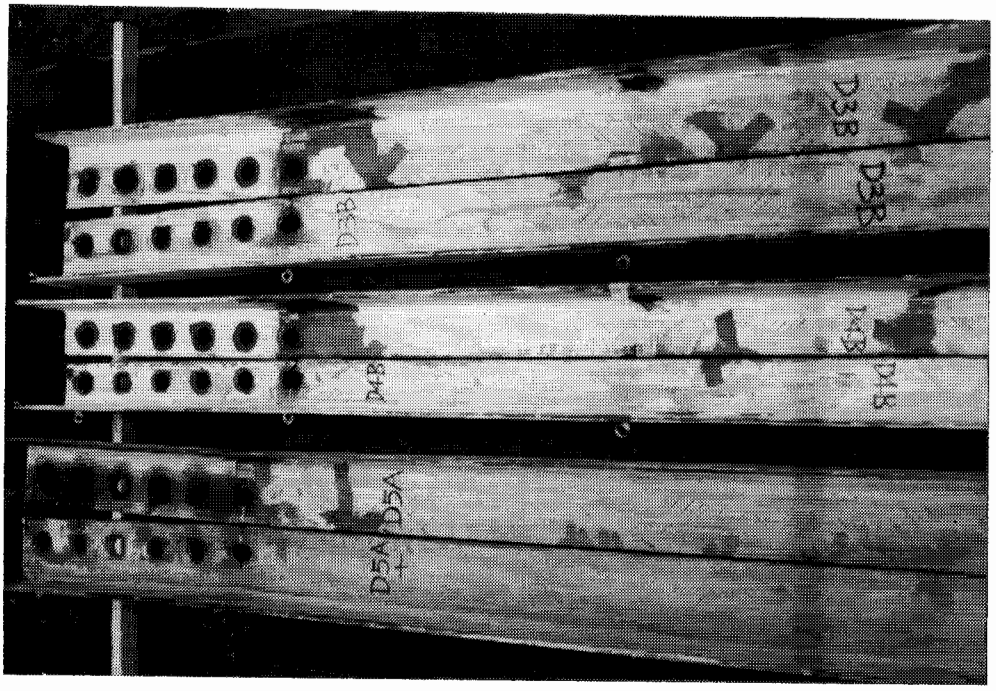

Figure 4.2 Deformed Double Angles

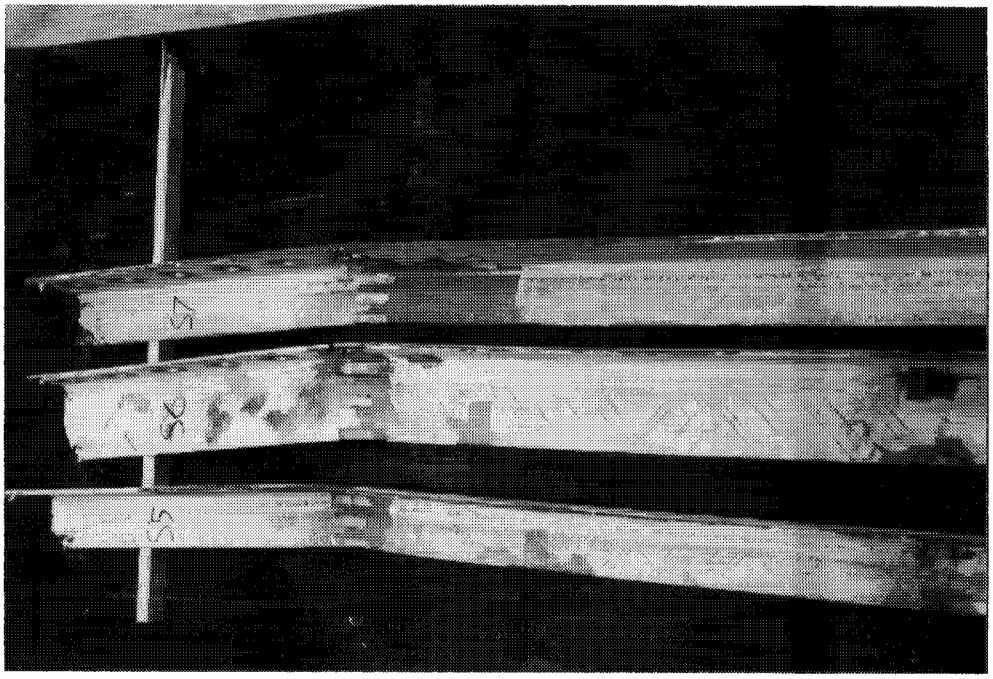

Figure 4.1 Deformed Single Angles

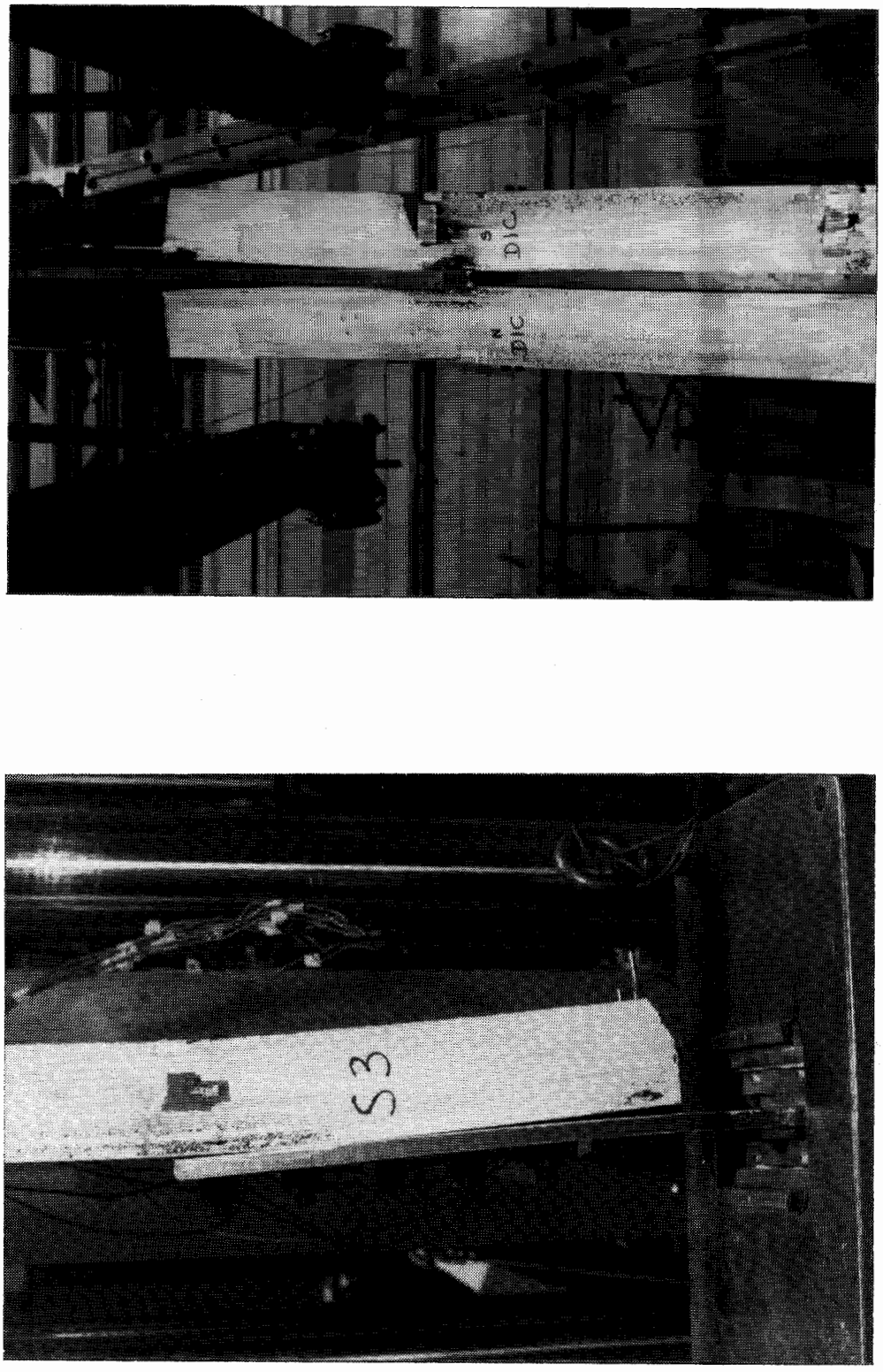

Figure 4.3 Global and Local Bending

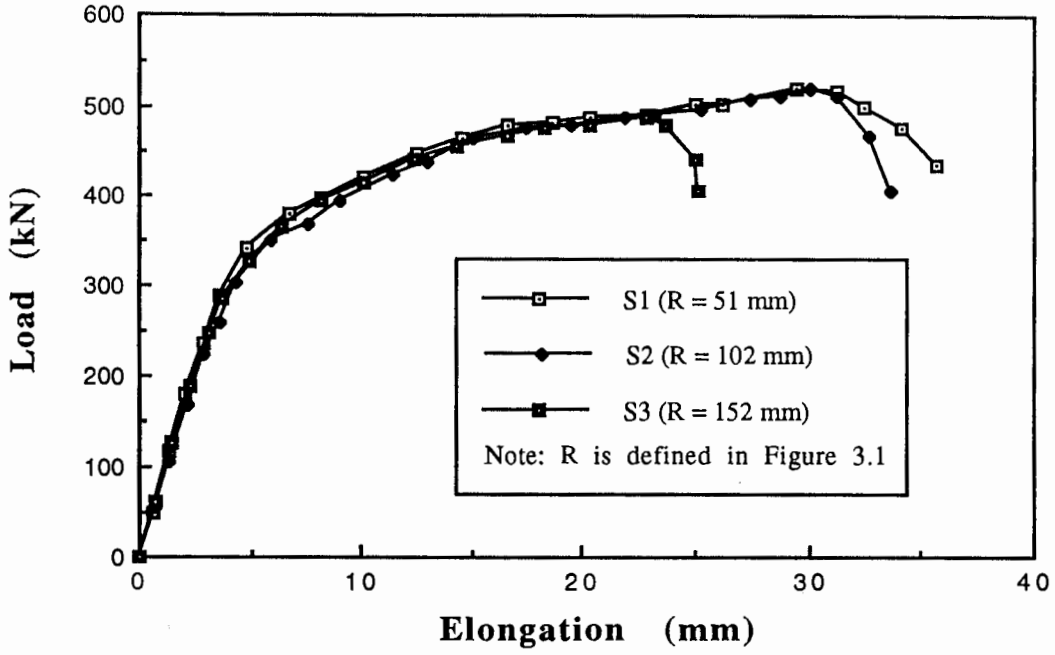

Figure 4.4 Load vs. Elongation for S1, S2, and S3

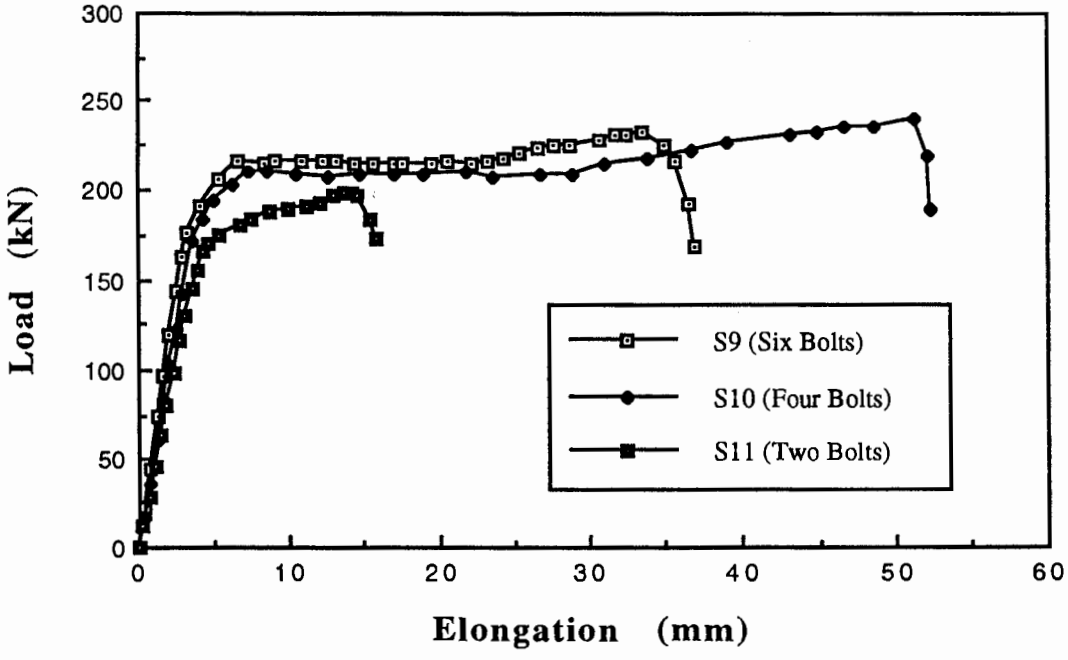

Figure 4.5 Load vs. Elongation for S9, S10, and S11

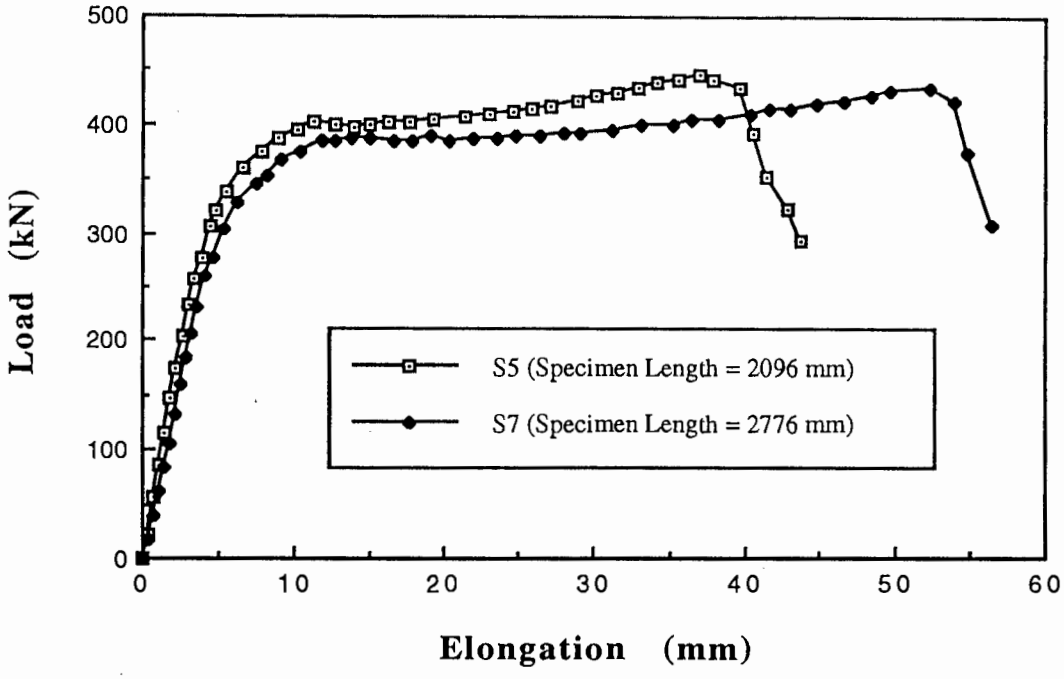

Figure 4.6 Load vs. Elongation for S5 and S7

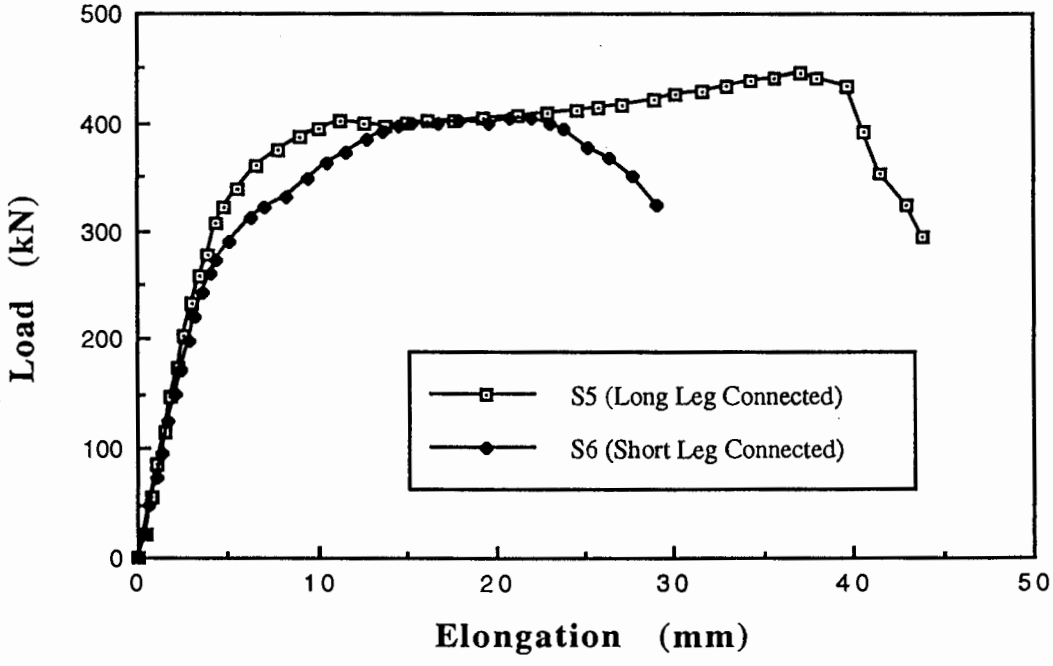

Figure 4.7 Load vs. Elongation for S5 and S6

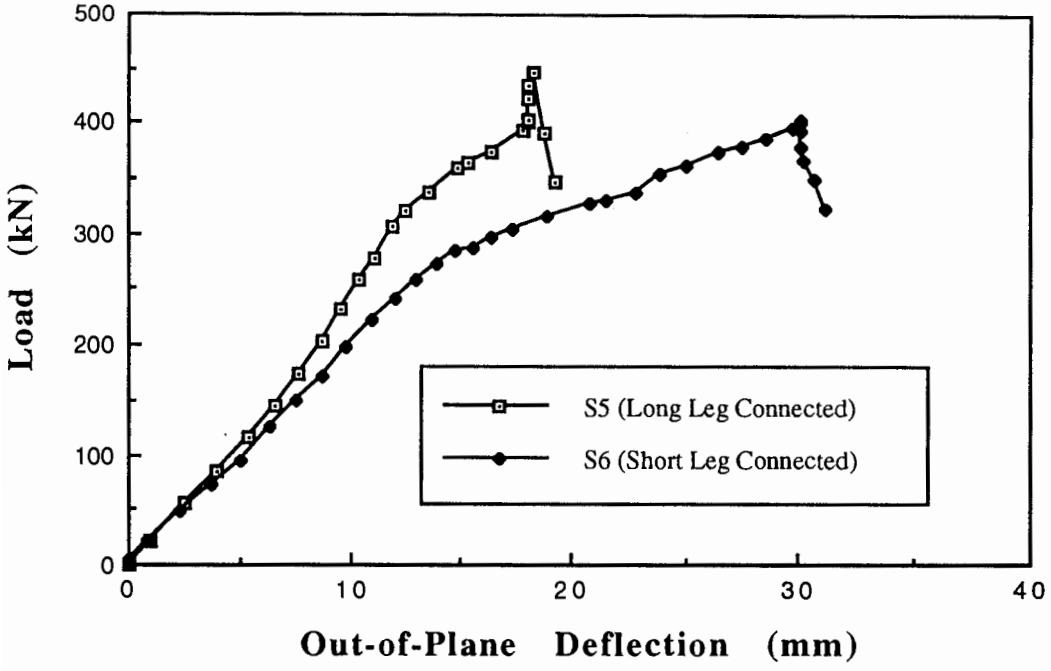

Figure 4.8 Load vs. Out-of-Plane Deflection for S5 and S6

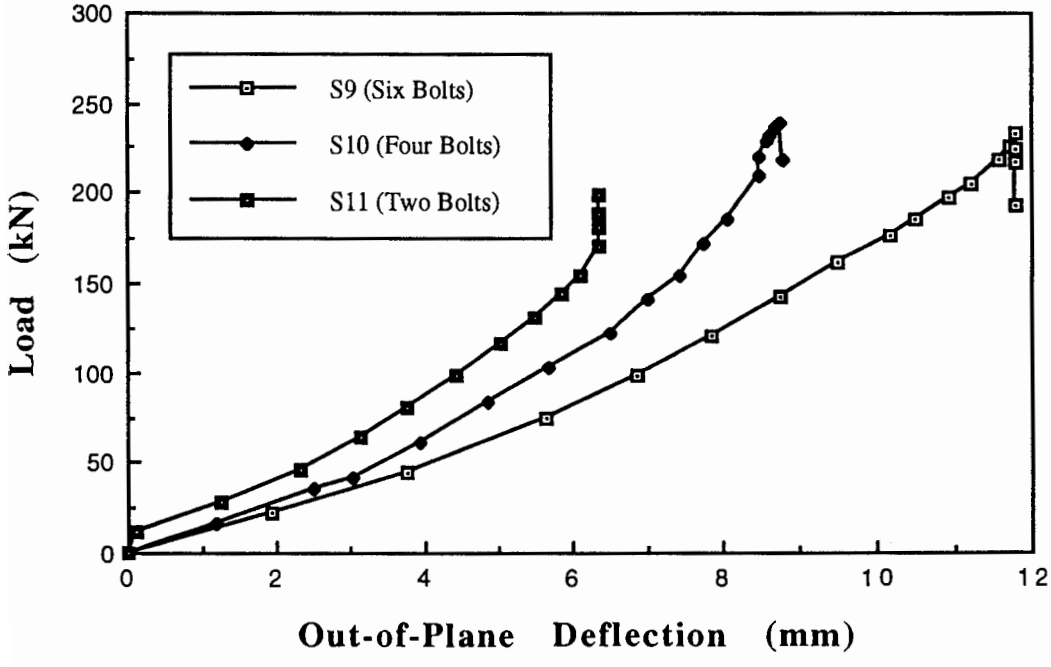

Figure 4.9 Load vs. Out-of-Plane Deflection for S9, S10, and S11

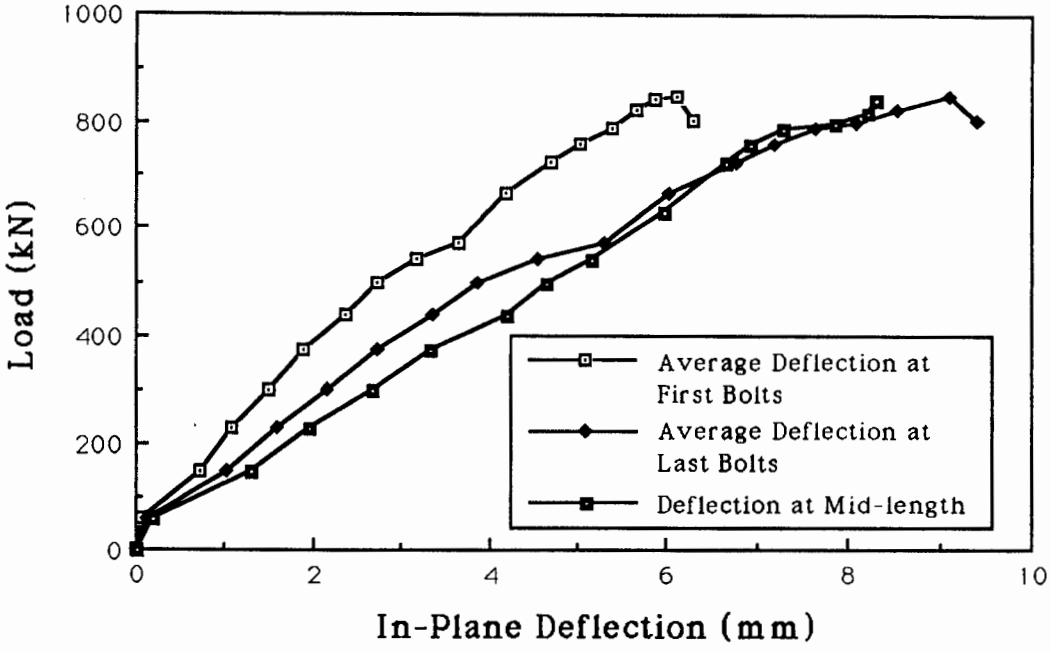

Figure 4.10 Load vs. In-Plane Deflection for D3-2

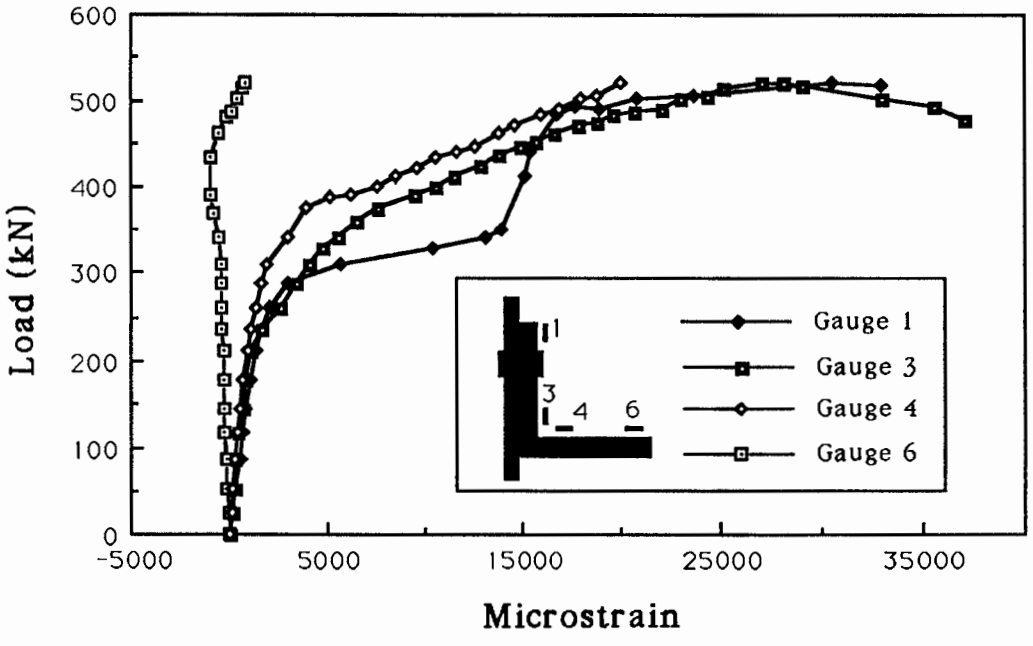

Figure 4.11 Load vs. Strain at the Critical Cross-Section for S1

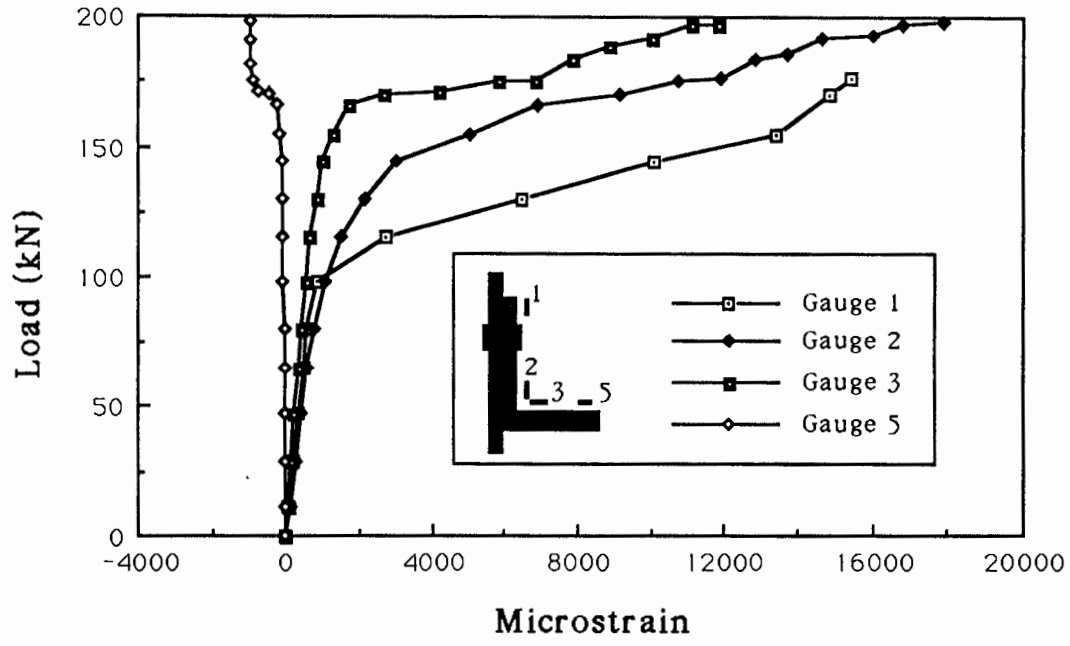

Figure 4.12 Load vs. Strain at the Critical Cross-Section for S11

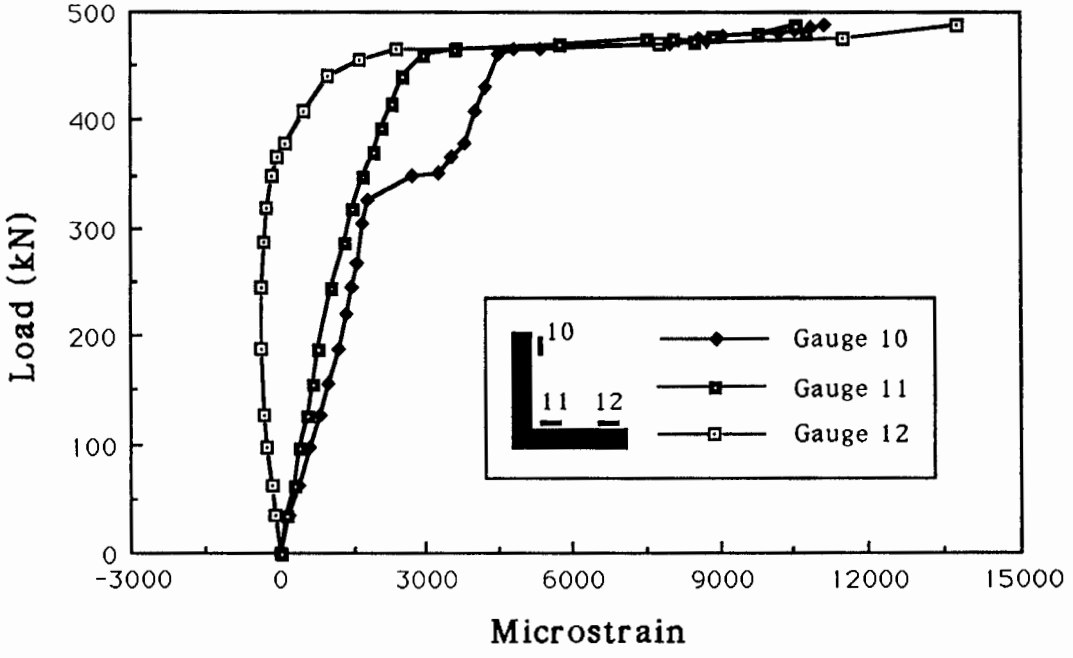

Figure 4.13 Load vs. Strain at the Mid-length Cross-Section for S3

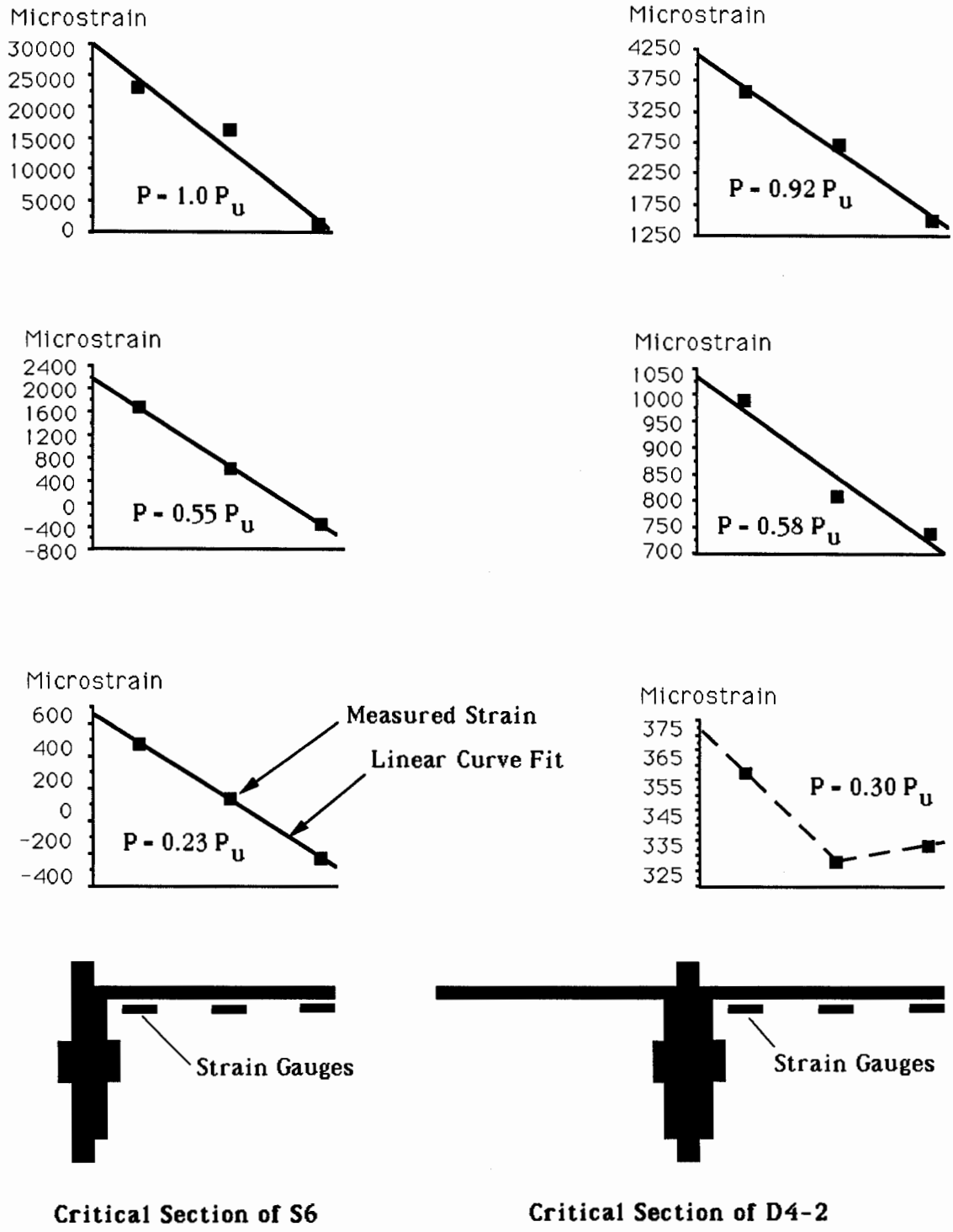

Figure 4.14 Strain Distribution Patterns for S6 and D4-2

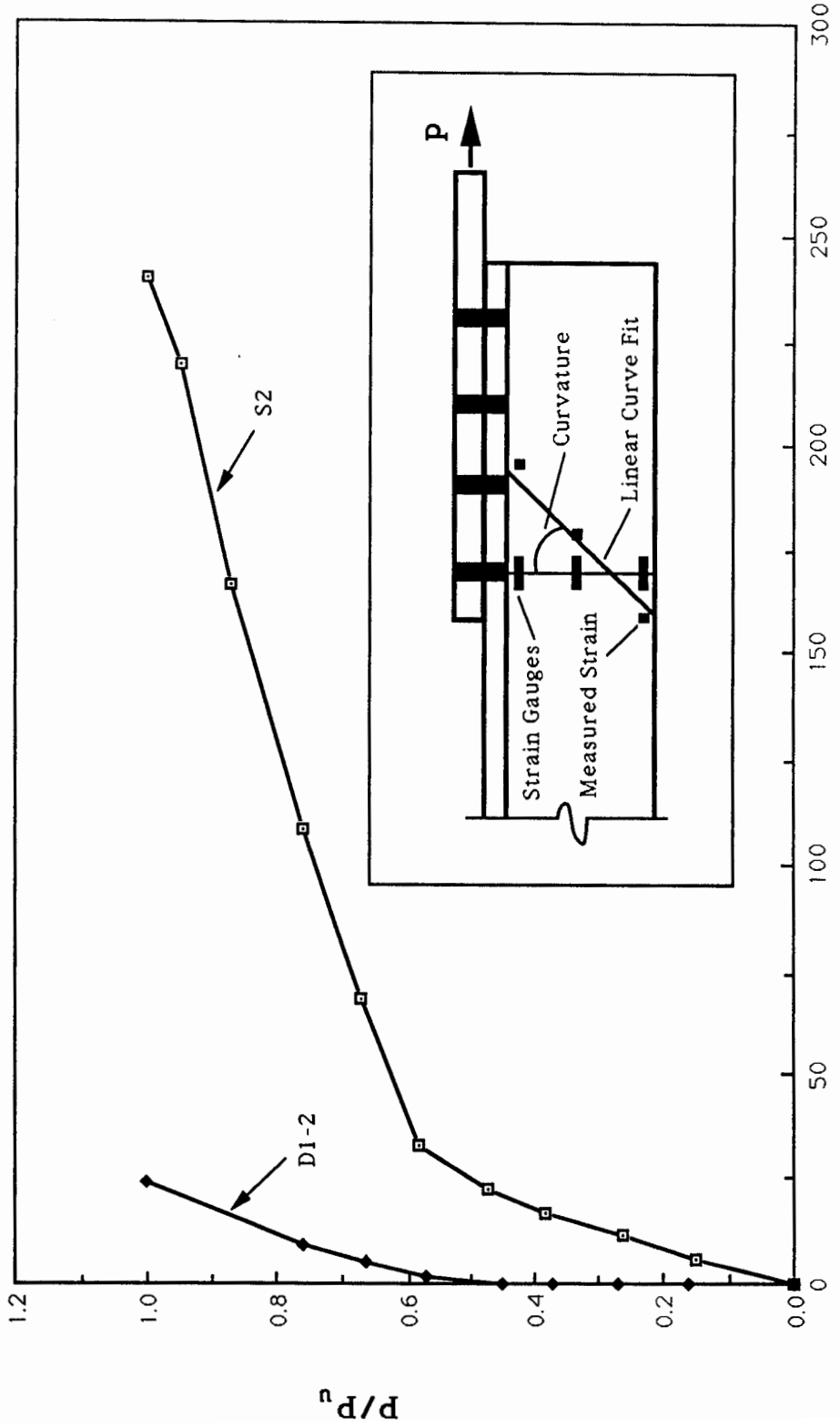

Figure 4.15 Load vs. Curvature for S2 and D1-2

5. Finite Element Analysis

5.1 General Background

The main goal of the finite element analysis was to evaluate the stress distribution of the critical cross-section at ultimate load. Five specimens chosen from the experimental program, S6, S11, D4-2, D7, and D9, were studied. It was found that the calculated ultimate strength of these specimens agreed well with the experimental results. Thus, finite element models can be used to predict the ultimate strength of angle members for purposes of parametric studies. In this project, a hypothetical specimen was modeled to obtain the ultimate load, thereby supplementing the data base of the experiment. The hypothetical specimen, designated as HD1, is a 152 x 102 x 7.9 double angle member with the short leg connected. This particular angle was chosen because it represents the largest difference in leg dimensions for available angle sections. The specimen length of HD1 is 2000 mm, and it is connected by four bolts at each end.

The commercial finite element program ANSYS (version 4.4) was used on a SUN workstation to perform the analysis. The problem was studied as a nonlinear load versus displacement analysis including plasticity and nonlinear effect of geometry. As a path-dependent nonlinear problem, the solution process requires a step-by-step incremental analysis. The Newton-Raphson solution method is used in the ANSYS program [29]. For this particular problem, the singularity of the stiffness matrix of the structure usually occurs after yielding. On a load versus elongation curve of the specimen, the singularity of the stiffness matrix is reflected by a flat plateau, that is, there is no increment of load as the elongation increases. In order to avoid the problem of the singularity, the displacement control method was used throughout the entire loading history of the analysis. The displacement control method produces a partitioned stiffness matrix which is no longer singular in most cases.

In the ANSYS program, the material properties are input as a stress versus strain curve that can be composed of up to five straight lines with different slopes. However, the descending part of the engineering stress versus strain curve is not accepted. In other words, a negative slope of the stress versus strain curve cannot be assigned.

5.2 Finite Element Model

A plastic quadrilateral shell element, ANSYS Element STIF43 [30], was used to model the angles. This element has six degrees of freedom at each of the four nodes. Modified extra displacement shapes are used for the in-plane effect. For the out-of-plane motion, a mixed interpolation of tensorial components is used. In the plane of the element,

a 2x2 lattice of integration points is used together with the Gaussian integration procedure. A five point rule is used through the thickness of the element. Shear deflections are included in this element. The gusset plates were modeled using an elastic quadrilateral shell element (ANSYS Element STIF63). The use of an elastic element for the gusset plates is based on the observation that there was no yielding in the gusset plates during the physical tests.

A typical mesh of the models is shown in Fig. 5.1. The coordinate system shown in Fig. 5.1 is the reference system used for descriptions that follow. To take advantage of the symmetry of the specimens, only one-half of the length of the member was modeled. At the mid-length cross-section of the member, the x-direction translational degrees of freedom and the y and z-direction rotational degrees of freedom were fixed. For double angle members, only one of the pair of angles was modeled because they are symmetrical about the gusset plate. The model used for double angle specimens differs from the single angle model merely in the boundary conditions of the gusset plate. In the model for double angle members, the gusset plate is constrained such that neither the z displacements nor the out-of-plane rotations (the x and y rotational degrees of freedom) can occur. However, the gusset plate of a single angle is free to have z displacements and out-of-plane rotations about the x and y axes. The longitudinal displacement, which is comparable to half of the total elongation measured in tests, was applied to the leading edge of the gusset plate. In order to model the boundary conditions as presented by the hydraulic grips in the second phase tests, at the leading edge of the gusset plate all degrees of freedom were restrained except the x displacements.

The shear deformation of the bolts was ignored. It was assumed that the load was transferred from the gusset plate to the angle fully by the bearing of the bolts. Hence, in the finite element models, one-half of the circumference of each bolt hole in the angle, which was supposed to bear against the bolt in the tests, was coupled with the opposite face of the corresponding bolt hole on the gusset plate for the x and y translational degrees of freedom. (This was done node by node.) It should be recalled that the bolts had been pretensioned before loading, and that the bolts were still tight after tests. Therefore, all nodes around the bolt holes of the angle were coupled with the corresponding nodes of the gusset plate for the z translational degrees of freedom, as well as the x and y rotational degrees of freedom. As observed in the experimental program, local bending took place during loading, i.e., the corner of the angle separated from the gusset plate in the region from the end of the angle to approximately the second or third bolt. In that zone where the local bending was observed to have taken place, the angle and the gusset plate were left uncoupled in the finite element model in order to allow the separation to take place. In the

other regions of the connection, where there was no observed separation in the tests, the z translational degrees of freedom were coupled between the corresponding nodes of the angle and the gusset plate in order to model the interaction between these two components.

The static material properties obtained from the coupon tests (Table 4.1) were used for the analysis of specimens S6, S11, D4-2, D7, and D9. For specimen HD1, the material properties were assigned as follows: elastic modulus (E) = 200 000 MPa; static yield strength (F_y) = 300 MPa; and static ultimate strength (F_u) = 450 MPa.

5.3 Analytical Results

In the analysis, the solution usually converged very slowly after yielding, and the increment for each load step had to be made very small. At a certain point, the analysis was terminated because the solution diverged even for an extremely small load increment. The analysis had never reached any unloading condition when it was terminated. The load which was obtained at the last converged load step was taken as the analytical ultimate load of the specimen.

Table 5.1 presents the summary of the analytical ultimate strength and shows a comparison with the experimental results. It can be seen that the finite element model is a good predictor of the physical tests: the mean value of the ratio of analytical ultimate load to the experimental value is 0.988, and the standard deviation and coefficient of variation of this value are 0.059 and 0.060, respectively. Therefore, the result of the hypothetical case (HD1) can be used with confidence.

The load versus elongation response obtained analytically can be compared with that observed in the experiment. The comparison for specimen D9 is plotted in Fig. 5.2, where it can be seen that the analytical curve is very similar to the test result. For other specimens, the analytical behavior also agrees with the test results in the general sense, except that the elongation reached at the limit point of the analytical curves may differ from that of the test results.

The contours of the longitudinal stress in the connection region of specimen D9 (76 x 51 x 4.8 angle, two bolt connection) are shown in Fig. 5.3 for the last load step. The stress contours were mapped by linear interpolation from the averaged nodal stresses. It can be seen that there is a compression zone in the outstanding leg, including a portion of the critical section. The specimen S11 (76 x 51 x 4.8 angle, two bolt connection) showed similar stress contours in the connection region, as did as D9. For the specimens with four or six bolt connections, either the compression zone in the outstanding leg was not at the critical section, or there was no compression zone on the outstanding leg at all.

The stress distribution at the critical cross-section was studied at the ultimate load for

each specimen examined analytically. It was observed that, on the critical section of the connected leg, the longitudinal stress was always equal to, or slightly greater than, the material strength of the specimen. The excess of the longitudinal stress over the material strength can be attributed to the effect of the biaxial tensile stresses. On the critical section of the outstanding leg the averaged longitudinal stress was about at the yield strength for the specimens with four or six bolt connections, but less than the yield strength for the specimens with two bolt connections.

It should be pointed out that the finite element models used for this analysis were constructed so that they would imitate the conditions of the physical tests carried out in this study. In the model, the load was assumed to transfer from the gusset plate to the angle in a way that is consistent with a bearing-type connection. The actual load transfer mechanism in a real connection may involve both friction and bearing. However, even in a friction-type connection, it is expected that the bolts will go into bearing before the member reaches its ultimate load.

In the finite element model, it was also assumed that the angle is connected to the gusset plate in such a way that these two components remain contact around the bolt holes during the entire loading history. This assumption is rational because the clamping force produced by the preloaded bolt should be sufficient to prevent the separation of these two components. Finally, it was assumed that the shear deformation of the bolts can be neglected. Further studies are recommended to verify the assumptions made in this finite element analysis.

Table 5.1 Summary of Analytical Results

Specimen	Size (mm)	Ultimate Load (kN)		A/E[2]
		Analysis	Experiment[1]	
S6	102 x 76 x 6.4	350.9	376.7	0.93
S11	76 x 51 x 4.8	172.2	185.4	0.93
D4-2	102 x 76 x 6.4	733.6	735.8	1.0
D7	76 x 51 x 4.8	415.4	389.4	1.07
D9	76 x 51 x 4.8	331.8	328.0	1.01
HD1	152 x 102 x 7.9	1218.0	N.A.	N.A.

Notes: 1. The experimental ultimate load is the static ultimate load (obtained at zero strain rate).
2. A/E is the ratio of the analytical ultimate load to the experimental ultimate load.

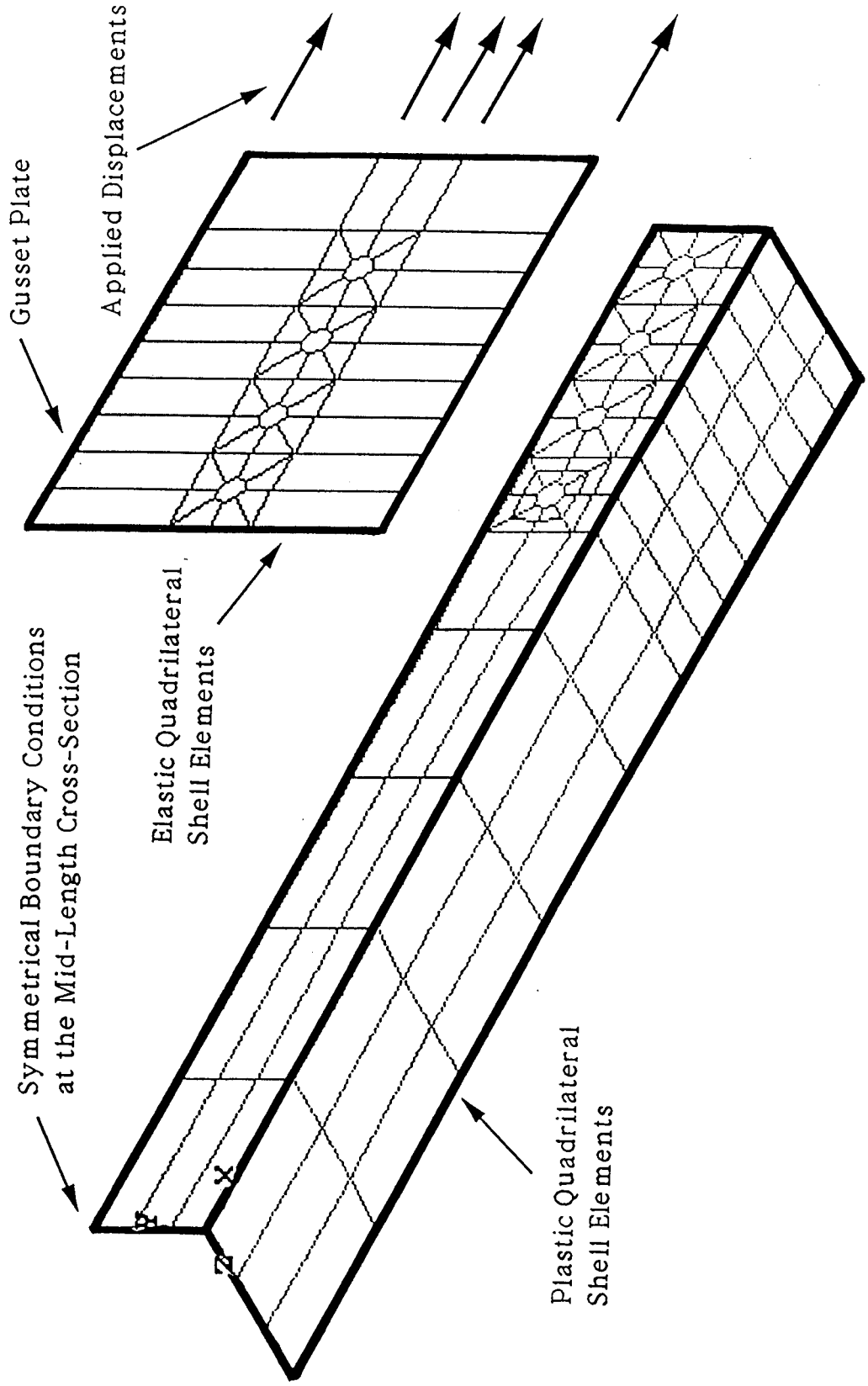

Figure 5.1 A Typical Mesh for the Finite Element Models

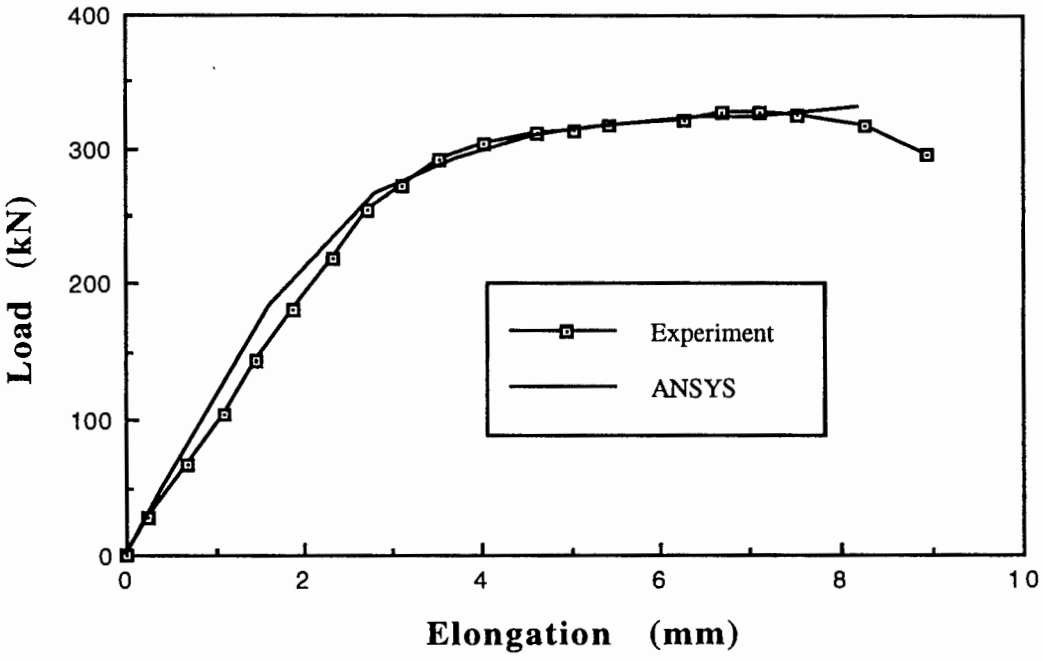

Figure 5.2 Comparison of Load vs. Elongation for D9

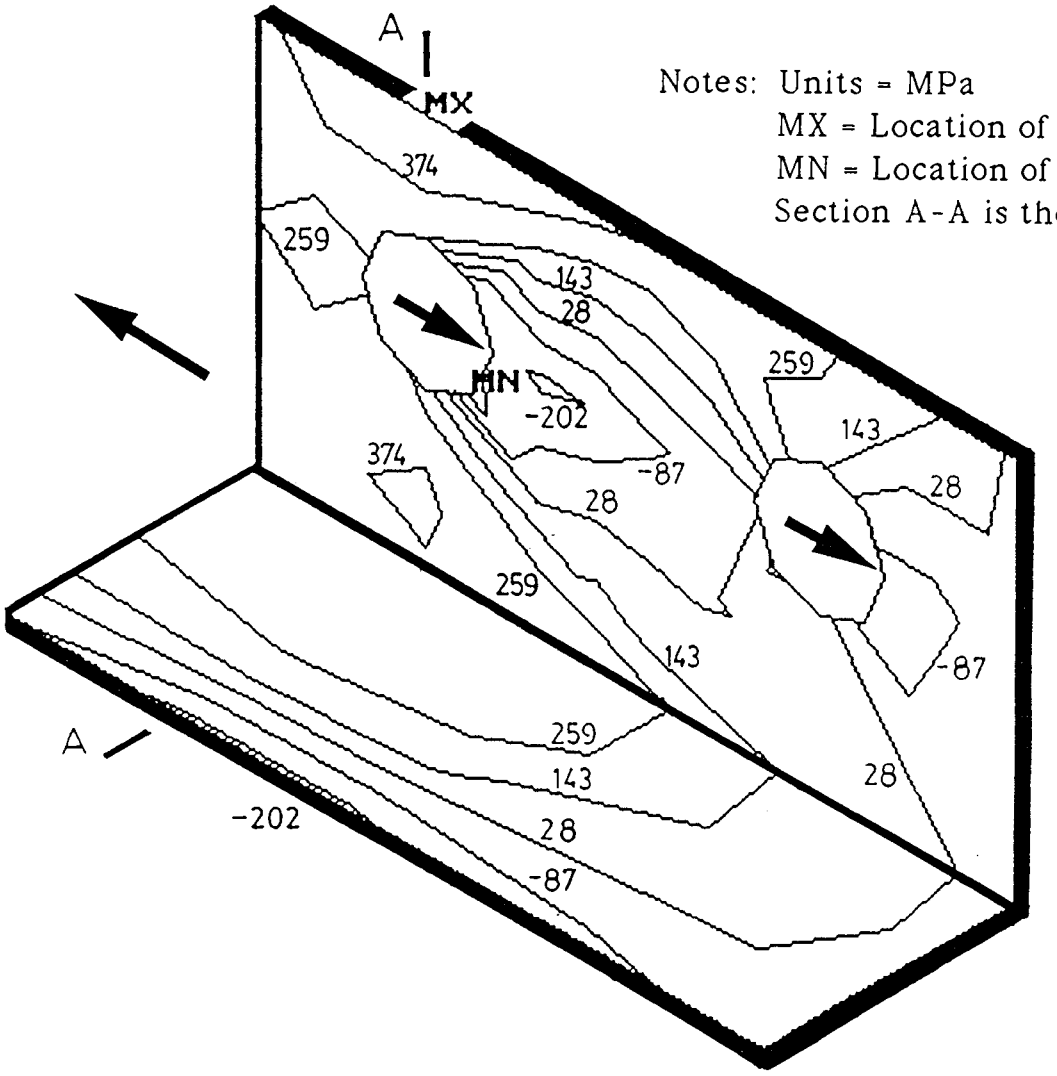

Notes: Units = MPa
MX = Location of Max. Stress
MN = Location of Min. Stress
Section A-A is the Critical Cross-Section

Figure 5.3 Stress Contours in the Connection Region of D9

6. Discussion

6.1 Introduction

In this chapter, the results obtained from both the experiment and the finite element analysis are discussed with respect to the test parameters (set out in Section 3.1) that were considered to have a possible effect on the net section strength. The $(1 - \frac{\bar{x}}{L})$ rule is examined for the particular case of single and double angle members by comparing it with the test results of this study and others. An alternative net section strength formula based on an assumed failure model is proposed. The current specifications are evaluated, and a new design provision is recommended.

6.2 Discussion of Test Results

6.2.1 Effect of Member Length

The test results indicate that, within the practical range, the net section strength of both single and double angle members is not affected by changes in the member length. As shown in Table 4.2, there is a negligible difference between the test efficiencies of S5 and S7, which were identical specimens (102 x 76 x 6.4 angles, six bolt connections) except that the member length of S7 (2776 mm) is 33 percent greater than that of S5 (2096 mm). Similarly, the difference in net section efficiency between D5 and the D3 specimens (D3-1 and D3-2) is also negligible, even though D5 (2776 mm) is 55 percent longer than the D3 specimens (1786 mm).

6.2.2 Effect of Out-of-Plane Constraint to a Single Angle

In a general sense, the amount of out-of-plane stiffness of the gusset plate reflects the degree of constraint applied to the end of the angle in the direction perpendicular to the plane of the gusset plate. The dimension "R" of a gusset plate (see Fig. 3.1) is related to the out-of-plane stiffness of the gusset plate for single angle members. A smaller value of R means a higher value of out-of-plane stiffness. Double angle members can be considered as the extreme case since the out-of-plane stiffness is infinity, or R is zero. The effect of out-of-plane stiffness of the gusset plate can be seen by studying the test results of the D1 specimens (D1-1, D1-2, and D1-3), and S1, S2, and S3. These specimens have values of R equal to zero (D1 specimens), or 51 mm, 102 mm, and 152 mm, respectively, for the S-series, while the other details are identical (102 x 102 x 6.4 angles, six bolt connections). The average test efficiency of the D1 series (R = 0) is 78.5 percent. For S1 (R = 51 mm), S2 (R = 102 mm), and S3 (R = 152 mm), the test efficiencies are 81.2 percent,

82.7 percent, and 77.6 percent, respectively. It can be seen that there is no significant difference in efficiencies among these specimens.

6.2.3 Effect of Angle Thickness

Specimen S8 (76 x 51 x 9.5 angle, six bolt connection) is similar to S9 (76 x 51 x 4.8 angle, six bolt connection) except that the angle thickness of S8 is twice that of S9. Specimens D6 and D7 have a similar relationship. By comparing the test efficiencies of these two pairs of angle members (see Table 4.2), it can be concluded that the angle thickness has little effect on the net section efficiency.

6.2.4 Effect of Angle Disposition

In this program, the 102 x 76 x 6.4 angle was designed to be connected by either the long leg (S5 and the D3 series) or the short leg (S6 and the D4 series). In all cases where the long leg of the angle is connected, the net section efficiency is higher than for the corresponding cases where the short leg is connected. S5 has a test efficiency that is ten percent higher than S6, and the efficiencies of the D3 series are seven percent higher than those of the D4 series, on average.

6.2.5 Effect of Connection Length

It was found that the net section efficiency is strongly affected by the connection length in certain ranges. For example, the single angle member S10 (76 x 51 x 4.8 angle) that has a four bolt connection has a test efficiency 21 percent higher than S11, which is the same angle but with a two bolt connection. For double angles, a specimen with a four bolt connection (D8) has a test efficiency that is 25 percent higher than the same pair of angles with a two bolt connection (D9). However, the difference in efficiency between the specimens with six bolt connections and those with four bolt connections is very small. For example, the difference between the test efficiencies of D7 (six bolt connection) and D8 (four bolt connection) is only three percent. It was observed in the finite element analysis that there is a compressive zone at the critical cross-section of the specimens with two bolt connections, but no compressive zone at the critical cross-section for the cases in which the specimens are connected by four or six bolts. It seems that for the specimens with fewer than four bolts per line in the connections, the net section efficiency is significantly lower than for those cases with four or more bolts per line in the connections. For the specimens with four or more bolts per line in the connections, the effect of connection length upon the net section strength is minor.

6.2.6 Comparison between Single and Double Angles

As observed in the tests, the difference in behaviour between single and double angle members is mainly reflected in the amount of lateral deflection perpendicular to the gusset plate, the strain distribution at the critical cross-section, and the amount of the bending curvature measured in the connected leg at the critical cross-section. However, the test efficiencies are generally about the same for comparable single and double angle members. The exception is that for the specimens with small cross-sections (76 x 51 x 4.8 and 76 x 76 x 4.8 angles), the single angle members have an efficiency that is from 12 to 15 percent higher than that of the corresponding double angle members. The comparison between the efficiencies of single and double angle members is tabulated in Table 6.1. The overall average efficiency of single angle members is seven percent higher than that of the double angles. Some previous studies [3, 4, 6, 11] also showed that the efficiencies of single and double angle members are close. Therefore, it can be concluded that the net areas of both single and double angle members in tension are not fully effective, and that the difference between the net section efficiencies of single and double angle members can be neglected in practice.

Intuitively, it would be expected that double angles are more efficient than a single angle. In the direction perpendicular to the gusset plate, the load is applied eccentrically with respect to the center of gravity of a single angle. However, in the case of a pair of angles, there is no eccentricity in this direction. Nevertheless, a comparison of the behavior of an individual angle of the double angle set with a single angle reveals that they are different only in the boundary conditions. The constraint provided by the gusset plate to the end of a single angle can be considered analogous to that of a series of springs oriented in the direction perpendicular to the gusset plate. A double angle member is then an extreme case of this condition: the springs are infinitely stiff because of the symmetry of the double angles about the gusset plate. In other words, the difference between a single angle and double angles is the degree of constraint applied by the analogous springs. It was shown in Section 6.2.2 that the degree of constraint does not have a significant influence on the net section strength. Moreover, because local bending exists, each angle of a double angle member bends about the bolt line on each side of the gusset plate so that they seem to act individually rather than as a rigid unit.

6.3 Net Section Strength Formulae

6.3.1 Evaluation of the $(1 - \bar{x}/L)$ Rule

In order to best examine the predictions of net section strength given by different formulae, the test data used hereafter are a collection of those reported in this study and those obtained by others. The sources of the test data can be seen in Fig. 6.1. Only the specimens that were associated with the net section failure mode are included. There are 97 specimens in total, among which 76 are single angle members and 21 are double angle members. (Angle members with lug angles have been excluded.) Of the 97 specimens, 81 were fabricated by punching the fastener holes and 13 by drilling the holes. (Although the fabrication method was not specifically mentioned by Nelson [10], it has been inferred that his specimens must have used drilled holes. According to the British standard of the time when Nelson's tests were conducted, the fastener holes should be drilled when using high-strength fitted bolts, which was what was used in Nelson's experiment.) There are three specimens [6] for which the fabrication method could not be determined from the available information. In the following discussion, it has been assumed that these three specimens used punched holes. This is a conservative assumption.

The proposal put forward by Munse and Chesson (Equation 2.3) for the calculation of the effective net area was based on a large number of tests. These included mostly truss-type tension members such as I-shapes and channels, but did include some single and double angles. In Eq. 2.3, the product of K_1, K_2, K_3, and K_4 is, indeed, the net section efficiency, U. The values of K_1 and K_3 are close to unity for most cases. Thus, according to the Munse and Chesson investigation, the net section strength can be predicted as

$$\begin{aligned} P_u &= K_2 K_4 A_n F_u \\ &= K_2 \left(1 - \frac{\bar{x}}{L}\right) A_n F_u \end{aligned} \qquad [6.1]$$

where P_u = predicted net section strength of the member

K_2 = 0.85 for members with punched holes

= 1.0 for members with drilled holes

$\bar{x}$ = distance from the face of the gusset plate to the center of gravity of the angle

L = connection length

A_n = net area calculated using the nominal fastener hole size

F_u = ultimate tensile strength of the material

The comparison between the predictions of Eq. 6.1 and the test results is plotted in

Fig. 6.1. (In Fig. 6.1, as well as in the two following figures, Fig. 6.2 and 6.3, the specimens are classified into three categories according to the number of fasteners per line in the connections. However, the horizontal coordinate is in a random order and it is not on the scale of the connection length.) On the whole, Eq. 6.1 is slightly unconservative; the average of the ratio of the predictions to the test results is 1.05, with a standard deviation of 0.13. Nevertheless, the prediction given by Eq. 6.1 is particularly unconservative for the specimens with drilled holes and for the specimens connected by fewer than four fasteners per line.

In many specifications, the punching effect upon the net section strength is accounted for by taking the hole diameter as 2 mm (or 1/16 in.) larger than the actual hole size when computing the net area, rather than multiplying by the fabrication factor ($K_2 = 0.85$), as proposed by Munse and Chesson. Thus, the net section strength of single and double angle members is often predicted as

$$P_u = (1 - \frac{\bar{x}}{L}) A_n F_u \qquad [6.2]$$

where A_n = net area calculated by taking the diameter of a fastener hole 2 mm (1/16 in.) larger than the actual size for both cases of drilled or punched holes. (According to the AISC codes, the width of a fastener hole should be taken as 2 mm (1/16 in.) larger than the nominal dimension whether it is punched or drilled. In CAN/CSA-S16.1-M89, this allowance may be waived for drilled holes.)

All other notations are defined the same as those in Eq. 6.1.

For those specimens cited in the examination of Eq. 6.1, the predicted results given by Eq. 6.2 are generally an overestimation; the average ratio of the predicted capacities to the test results is 1.19 and the standard deviation is 0.13. The discrepancy between the results of Eq. 6.1 and Eq. 6.2 must be attributed to the inconsistent ways of including the punching effect. Calculation of the net areas of a wide selection of angle sections shows that the reduction of net area is less than four percent when the hole diameter is taken as 2 mm larger than the nominal size. For angles of large and medium sizes, the reduction is usually below two percent. These amounts of reduction are certainly not enough to be equivalent to the results obtained if the fabrication factor of 0.85 is used.

Based on the discussion above, it is concluded that the prediction given by Eq. 6.1 is slightly unconservative when it is used to predict the tensile capacity of single and double angle members. However, the exclusion of the fabrication factor (K_2) from Eq. 6.1

(which leads to Eq. 6.2), as is done in some of the specifications, will produce a significantly unconservative prediction. It is difficult to say whether the method of Eq. 6.1 or 6.2 is more appropriate to estimate the punching effect. However, it can be concluded that the fabrication factor (K_2) should be used together with the shear lag factor in Eq. 6.1.

6.3.2 Proposed Net Section Strength Formula

A failure model is proposed herein to provide an alternative formula to predict the net section strength of single or double angle members in tension. In the finite element analysis, it was found that at failure the average stress at the critical section of the connected leg reaches about the ultimate strength of the material. It was also observed that at failure the average stress at the critical section of the outstanding leg is at about the yield strength for the specimens with four or more bolts per line in the connections, but less than the yield strength for the specimens with a shorter connection length. Thus, in this failure model it is assumed that the critical section of the connected leg always develops the ultimate tensile stress, which is uniformly distributed. The longitudinal stress at the critical section of the outstanding leg is equivalent to a uniform tensile stress distribution with the stress value equal to the yield strength if the connection has four or more fasteners per line. If there are fewer than four fasteners per line in the connection, the stress level in the outstanding leg must be modified in order to account for the effect of connection length. After studying the available test results of the specimens with two or three fasteners per line in the connections, it is recommended that one-half of the yield stress be used in the outstanding leg for these cases. The net section capacity of single and double angle members based on this failure model would be the ultimate strength of the critical section of the connected leg plus the strength contributed by the critical section of the outstanding leg. It is given by the following formula:

$$P_u = F_u A_{cn} + \beta F_y A_o \qquad [6.3]$$

where P_u = predicted net section strength of the member

F_u = ultimate strength of the material

F_y = yield strength of the material

A_{cn} = net area of the connected leg at the critical cross-section, computed by taking the diameter of holes 2 mm (1/16 in.) larger than the nominal size

A_o = gross area of the outstanding leg

β = 1.0 for members with four or more fasteners per line in the connection

= 0.5 for members with fewer than four fasteners per line in the connection

Alternatively, the net section strength can be written using the effective net area as

$$P_u = F_u (A_{cn} + ß \frac{F_y}{F_u} A_o) \qquad [6.3a]$$

in which the effective net area of the angle is defined as the sum inside the parentheses. Based on Eq. 6.3a, the net section efficiency is

$$U = \frac{A_{cn} + ß \frac{F_y}{F_u} A_o}{A_n} \qquad [6.4]$$

In Fig. 6.2, the net section strength predicted by using Eq. 6.3 is compared with the test results that were used in the comparisons with Eq. 6.1 and 6.2. The average ratio of the predicted values to the test results is 0.96, with a standard deviation of 0.08. This indicates that Eq. 6.3 provides a conservative prediction and one which falls in a narrower scatter band than did the predictions obtained using Eq. 6.1. Eq. 6.3 can, therefore, be used to predict the net section strength of single and double angle members with bolted or riveted connections.

6.4 Evaluation of Current Specifications

6.4.1 The AASHTO and AREA Specifications

Obviously, the specifications of AASHTO [22] and AREA [23], which define the net area as fully effective when calculating the net section strength of double angle members, are inconsistent with the results obtained from this program and other studies. These specifications overestimate the net section strength of double angle members by anywhere from 10 to 40 percent. For single angle members, the approach of AASHTO and AREA is in a format similar to that of Eq. 6.3a, that is, the effective net area is taken as the net area of the connected leg plus a portion of the gross area of the outstanding leg. However, the AASHTO and AREA codes fail to recognize the effect of connection length, which, in this study, has been found to cause a difference in the net section efficiency of up to 25 percent. In comparison with Eq. 6.3a, the AASHTO and AREA codes are conservative for single angles, provided that the connection has four or more fasteners per line. However, they are unconservative for single angles connected by fewer than four fasteners per line. For example, for angles of ASTM A36 steel connected by fewer than four fasteners per line, the net area defined by Eq. 6.3a is the net area of the connected leg plus 31 percent of the area of the outstanding leg, which is less than that specified in the AASHTO and AREA

codes. These specifications would use 50 percent of the area of the outstanding leg.

6.4.2 The AISC Codes and CAN/CSA-S16.1-M89

The current AISC codes [16, 24] and CSA Standard CAN/CSA-S16.1-M89 [21] for angle members were derived from Eq. 6.2. However, it was considered that Eq. 6.2 is inconvenient for direct application in practical designs. To design a tension member for a given load, for example, a shape must first be selected by judgement, and the connection must then be designed based on the trial shape in order that the net section efficiency ($U = 1 - \frac{\bar{x}}{L}$) can be computed. The net section strength obtained for this trial shape must be examined. If the strength is inadequate or excessive, the designer has to select another shape. It will usually take a few iterations to find a suitable shape.

To simplify the design procedure, a Task Committee of AISC derived the reduction coefficients from Eq. 6.2 [31]. The reduction coefficients they proposed are those that have been adopted for use in the current AISC codes and CAN/CSA-S16.1-M89. About 120 hypothetical cases of tension members, including single angle members with one leg connected and I-shape members with two flanges connected, were studied in order to derive the reduction coefficients. The angle members consisted of equal leg angles and unequal leg angles with either the long leg or short leg connected. The grades of angle steel and the types of bolts were combined in the following ways:

1. ASTM A36 steel angle with 22 mm dia. A325 friction-type bolts;
2. ASTM A36 steel angle with 22 mm dia. A325 bearing-type bolts;
3. ASTM A572 Grade 65 steel angle with 22 mm dia. A490 friction-type bolts;
4. ASTM A572 Grade 65 steel angle with 22 mm dia. A490 bearing-type bolts.

The I-shape members were all of ASTM A36 steel; and the fasteners for I-shape members were 22 mm dia. A325 bolts in both friction-type and bearing-type connections.

The ($U = 1 - \frac{\bar{x}}{L}$) rule was applied to each case, with the number of bolts in the connection chosen according to the yield strength of the gross cross-section of the member. The calculated net section efficiencies ranged from 0.685 to 0.970, with a mean of 0.86 for angle members with three or more bolts per line in the connections, and from 0.670 to 0.967 for I-shape members, with a mean of 0.86. For angle members with two bolts per line in the connections, the calculated efficiencies were as low as 0.587. As a consequence of this examination, the angle members (both single and double angles) were assigned a reduction coefficient of 0.85 if the connections included three or more bolts per line, and 0.75 for the members with two bolts per line in the connections. These reduction

coefficients, derived from Eq. 6.2, are essentially the mean of the net section efficiencies examined. Because Eq. 6.2 overestimates the net section strength, the prediction according to the AISC codes and CAN/CSA-S16.1-M89 is, consequently, unconservative. In Fig. 6.3 the predicted net section capacities based on the AISC codes and CAN/CSA-S16.1-M89 are compared with the test results. (The net areas were computed according to the AISC rules, that is, the width of a fastener hole is taken 2 mm larger than the nominal dimension in all cases.) The average ratio of the predictions to the test results is 1.12, with a standard deviation of 0.17. The prediction is especially unconservative for the members with two or three bolt connections. Some predicted values are greater than the test results by about 50 percent.

6.5 Recommended Design Method

For a given angle section, the net section strength can be calculated according to Eq. 6.3. In a format consistent with that of CAN/CSA S16.1-M89, the factored resistance (T_r) of the net section will be

$$T_r = 0.85\,\emptyset\,(F_u\,A_{cn} + \beta\,F_y\,A_o) \qquad [6.5]$$

where Ø, a resistance factor, = 0.90. In order to account for the fact that net section fracture occurs with little deformation, and, therefore, with little warning of failure, 0.85 is used in Eq. 6.5 to increase the safety index [31]. (The other symbols in Eq. 6.5 have been defined in Eq. 6.3.)

When choosing an angle section for a given load, Eq. 6.5 is inconvenient for use because the section has to be selected by trial. Thus, it is desirable to derive reduction coefficients from Eq. 6.4. In order to derive the reduction coefficients, angle members of CAN/CSA G40.21-M 300W steel or ASTM A36 steel were examined for each of the following types of connections:

1. A325 bolts in a bearing-type connection (threads intercepted);
2. A325 bolts in a friction-type connection (class A surfaces);
3. A490 bolts in a bearing-type connection (threads intercepted);
4. A490 bolts in a friction-type connection (class A surfaces);

The diameter of the bolts was taken as the maximum bolt size permissible for the width of the connected leg of the angle. This gives conservative results; it can be shown that for the same angle section, the value of U decreases according to Eq. 6.4 as the bolt size increases. For bolts in a bearing-type connection, it was considered that the threads are intercepted. This is common in practice; the length of the bolts used to connect angles

is usually so short that the threads are likely intercepted by the shear plane. Class A surfaces are the usual case for a friction-type connection. The number of bolts was determined in such a way that the factored resistance of the connection is not less than the factored resistance of the member, which is the least of the factored yield strength of the gross area and the factored net section strength calculated in accordance with Eq. 6.5. For angle sections with the connected leg width not less than 125 mm, the bolts can be arranged in either one or two lines, while only one line of bolts is used if the connected leg width is less than 125 mm. The value of ß is determined according to Eq. 6.3 so that the value of U in Eq. 6.4 is only a function of the cross-sectional properties of the angle sections. (It should be pointed out again that block shear type failures are not considered in this report.)

All the angle sections listed in *Handbook of Steel Construction* [32], excluding those that are too small to be connected by structural size bolts, were studied. In the case of unequal leg angles, it was considered that connection could be either by the long leg or by the short leg. Impractical cases must be eliminated. Specifically, for those angle sections that are so large that it is impossible to connect them by fewer than four bolts per line, the case of ß = 0.5 is excluded. Likewise, the case of ß = 1.0 is excluded if the angle section is so small that there is no reason to use more than three bolts per line in the connection. Considering all the cases described, and the limitations just noted, a total of 147 angle sections were examined for about 1500 cases. The net areas in Eq. 6.4, A_{cn} and A_n, were computed by taking the hole diameter 2 mm larger than the nominal hole size, which, in turn, is 2 mm larger than the bolt diameter. Table 6.2 presents the calculated net section efficiencies that were obtained by applying Eq. 6.4 to all the cases examined.

Because the width of a fastener hole may be taken as its nominal dimension if the hole is drilled, as specified in CAN/CSA-S16.1-M89, the net section efficiencies were recalculated for the angles of 300W steel using the nominal hole dimensions (the bolt diameter plus 2 mm). It was found that the increases of the net section efficiencies are always less than one percent for the case of ß = 1.0, and never greater than two percent for ß = 0.50. Thus, the net section efficiency can be considered as the same whether the fastener holes are punched or drilled.

As can be seen in Table 6.2, the range of the calculated net section efficiencies is relatively small. The calculated net section efficiencies are basically the same for different types of connections. According to Eq. 6.4, the value of U increases as the ratio of yield strength to ultimate strength, F_y/F_u, increases. However, the difference in the calculated net section efficiencies is insignificant when comparing angles of 300W steel and A36 steel. As mentioned before, the diameter of bolts had been taken as the maximum permissible size for the angle examined. Nevertheless, for angles of large sizes, the

diameter of bolts chosen in this way is excessively large as compared with the size of bolts used to connect angles in practical cases. It was found that, if 22 mm dia. bolts, which is a more common size of bolts used in practice, are chosen for the examination, the mean values of the calculated net section efficiencies in Table 6.2 will increase 0.01 to 0.02 for all the cases. It should also be noticed that the original equation, Eq. 6.3, is on the conservative side; the average ratio of its predictions to the test results is 0.96, with a standard deviation of 0.08. Thus, it is considered appropriate that the calculated net section efficiencies presented in Table 6.2 be rounded to the nearest higher five percent increment.

As a result of the above examination, it is recommended that for single and double angle members made of CAN/CSA 300W steel or ASTM A36 steel, the effective net area (A_{ne}) can be calculated as

$$A_{ne} = U A_n \qquad [6.6]$$

where U = 0.80 if the connection has four or more fasteners per line
= 0.60 if the connection has fewer than four fasteners per line
A_n = net area of the critical cross-section, calculated by taking the hole diameter 2 mm larger than the nominal size

Eq. 6.6 will give conservative results if it is applied to angles made of other types of steel for which the ratio of yield strength to ultimate strength is not less than that of ASTM A36 steel, that is, 0.62. In other words, Eq. 6.6 can be used conservatively for angles made of all steels commonly available in North America.

Finally, using the effective net area obtained from Eq. 6.6, the factored resistance of the net section can be calculated as

$$T_r = 0.85 \, \phi \, F_u \, A_{ne} \qquad [6.7]$$

It should be pointed out that in all the equations proposed the net areas should be calculated according to the $s^2/4g$ rule if there is more than one line of bolts and the holes are staggered. If drilled fastener holes are known to be used, the net areas may be computed using the nominal hole dimension as specified in CAN/CSA-S16.1-M89, if desired.

In Fig. 6.4 Eq. 6.6 is examined using the test results which had been used to examine Eq. 6.3. It was found that the average ratio of the predictions based on Eq. 6.6 to the test results is 0.97, with a standard deviation of 0.10, and nearly all the ratios are below 1.10. (It is unconservative if the ratio is greater than 1.0.) There are a few exceptional cases, in which the values of the ratio can be as high as about 1.20. The specimens related to these

relatively high ratios were tested in Britain, and all of them were connected by the short legs. The difference between the widths of the connected leg and the outstanding leg of these specimens is greater than for any unequal leg angle section available in North America. Therefore, it can be concluded that the net section strength can be predicted well either using Eq. 6.3 directly or based on the effective net area given by Eq. 6.6. Designers can be given the option of using either Eq. 6.5 or Eq. 6.7 to calculate the factored tensile resistance of a net section.

Table 6.1 Comparison of Efficiencies between Single and Double Angles

Specimen		Size (mm)	Efficiency, U (%)		S/D[1]
Single Angle	Double Angles		Single Angle	Double Angles	
S1, S2, S3	D1-1, D1-2, D1-3	102 x 102 x 6.4	80.5	78.5	1.03
S4	D2	76 x 76 x 4.8	92.5	81.8	1.13
S5	D3-1, D3-2	102 x 76 x 6.4	92.5	87.6	1.06
S6	D4-1, D4-2	102 x 76 x 6.4	84.5	82.0	1.03
S7	D5	102 x 76 x 6.4	90.4	89.5	1.01
S8	D6	76 x 51 x 9.5	90.3	89.5	1.01
S9	D7	76 x 51 x 4.8	90.4	86.3	1.12
S10	D8	76 x 51 x 4.8	100	89.7	1.12
S11	D9	76 x 51 x 4.8	82.5	71.8	1.15
Average, All Specimens			88.3	83.3	1.07

Note: 1. $S/D = \frac{\text{efficiency of single angles}}{\text{efficiency of double angles}}$

Table 6.2 Calculated Net Section Efficiencies

Case Examined	Four or More Bolts per Line			Fewer than Four Bolts per Line		
	Range	Mean	Standard Deviation	Range	Mean	Standard Deviation
300W Steel A325 Bolts Bearing-type	0.75 ⇒0.86	0.79	0.03	0.51 ⇒0.72	0.60	0.05
300W Steel A325 Bolts Friction-type	0.75 ⇒0.86	0.80	0.03	0.52 ⇒0.72	0.61	0.05
300W Steel A490 Bolts Bearing-type	0.75 ⇒0.86	0.79	0.03	0.50 ⇒0.72	0.60	0.05
300W Steel A490 Bolts Friction-type	0.75 ⇒0.86	0.79	0.03	0.52 ⇒0.72	0.60	0.05
A36 Steel A325 Bolts Bearing-type	0.71 ⇒0.84	0.76	0.03	0.49 ⇒0.71	0.58	0.05
A36 Steel A325 Bolts Friction-type	0.71 ⇒0.84	0.77	0.03	0.50 ⇒0.71	0.59	0.05
A36 Steel A490 Bolts Bearing-type	0.71 ⇒0.84	0.76	0.03	0.49 ⇒0.71	0.58	0.05
A36 Steel A490 Bolts Friction-type	0.71 ⇒0.84	0.76	0.03	0.50 ⇒0.71	0.59	0.05
All Cases	0.71 ⇒0.86	0.78	0.03	0.49 ⇒0.72	0.59	0.05

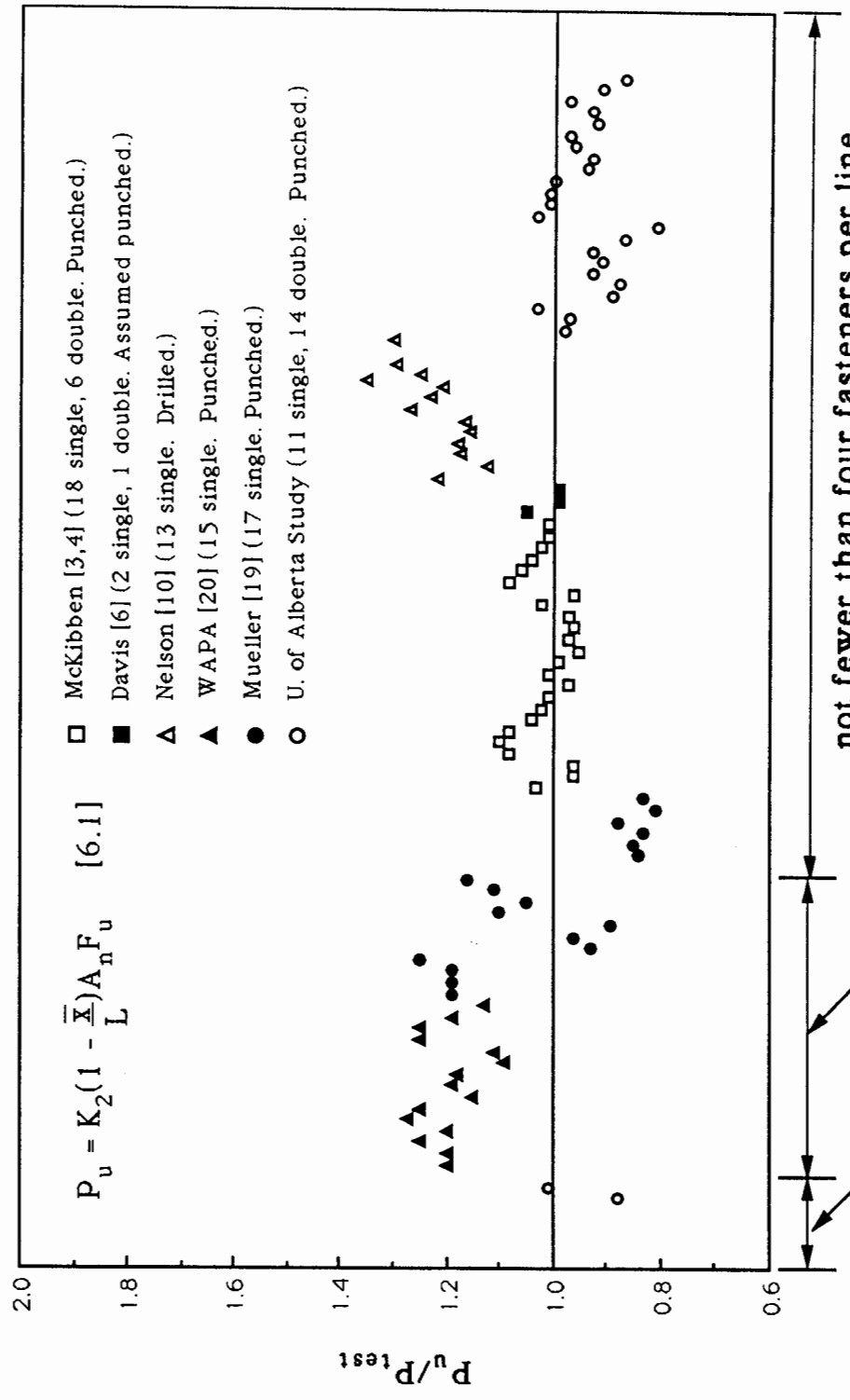

Figure 6.1 Evaluation of Eq. 6.1

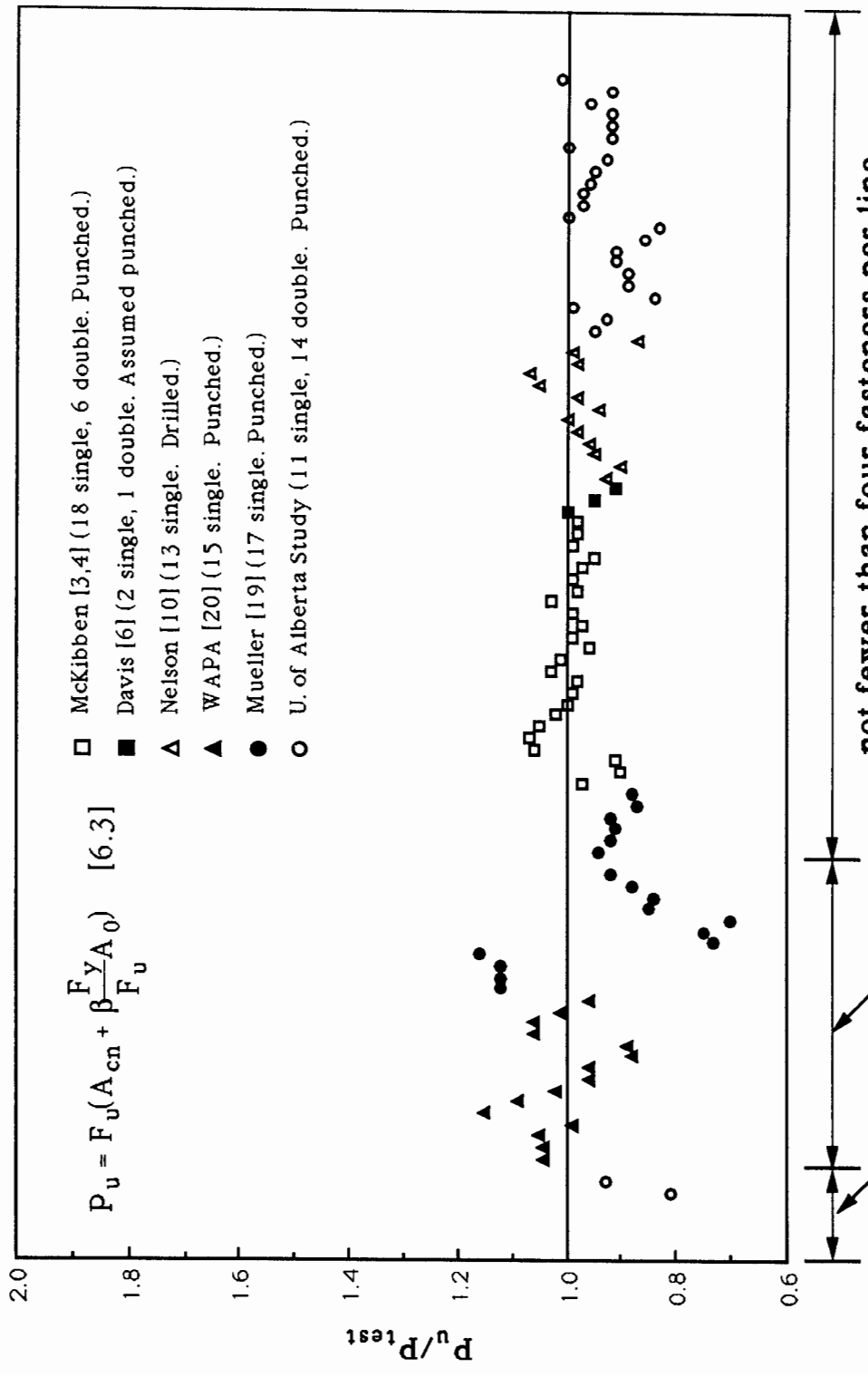

Figure 6.2 Evaluation of Eq. 6.3

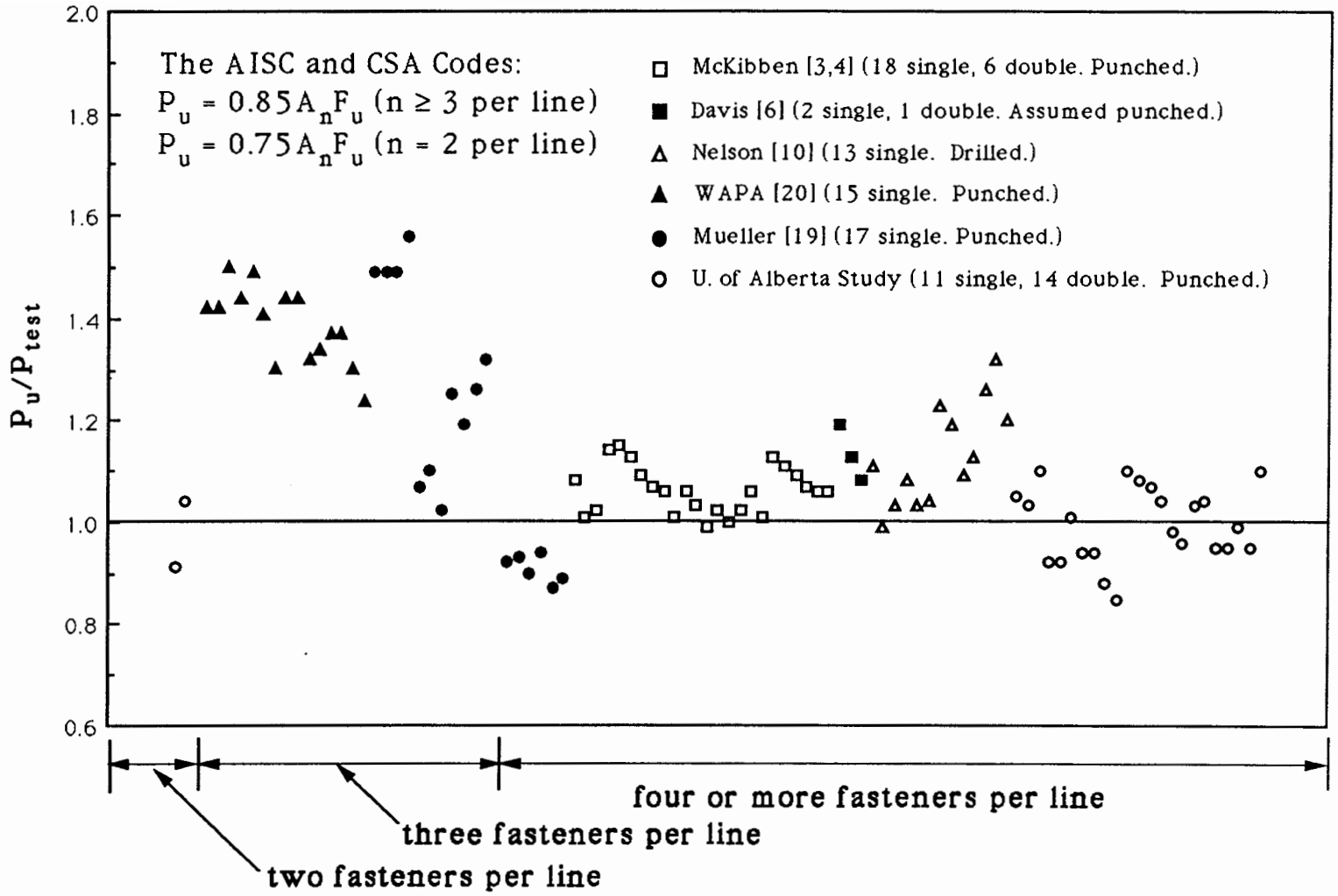

Figure 6.3 Evaluation of the AISC and CSA Specifications

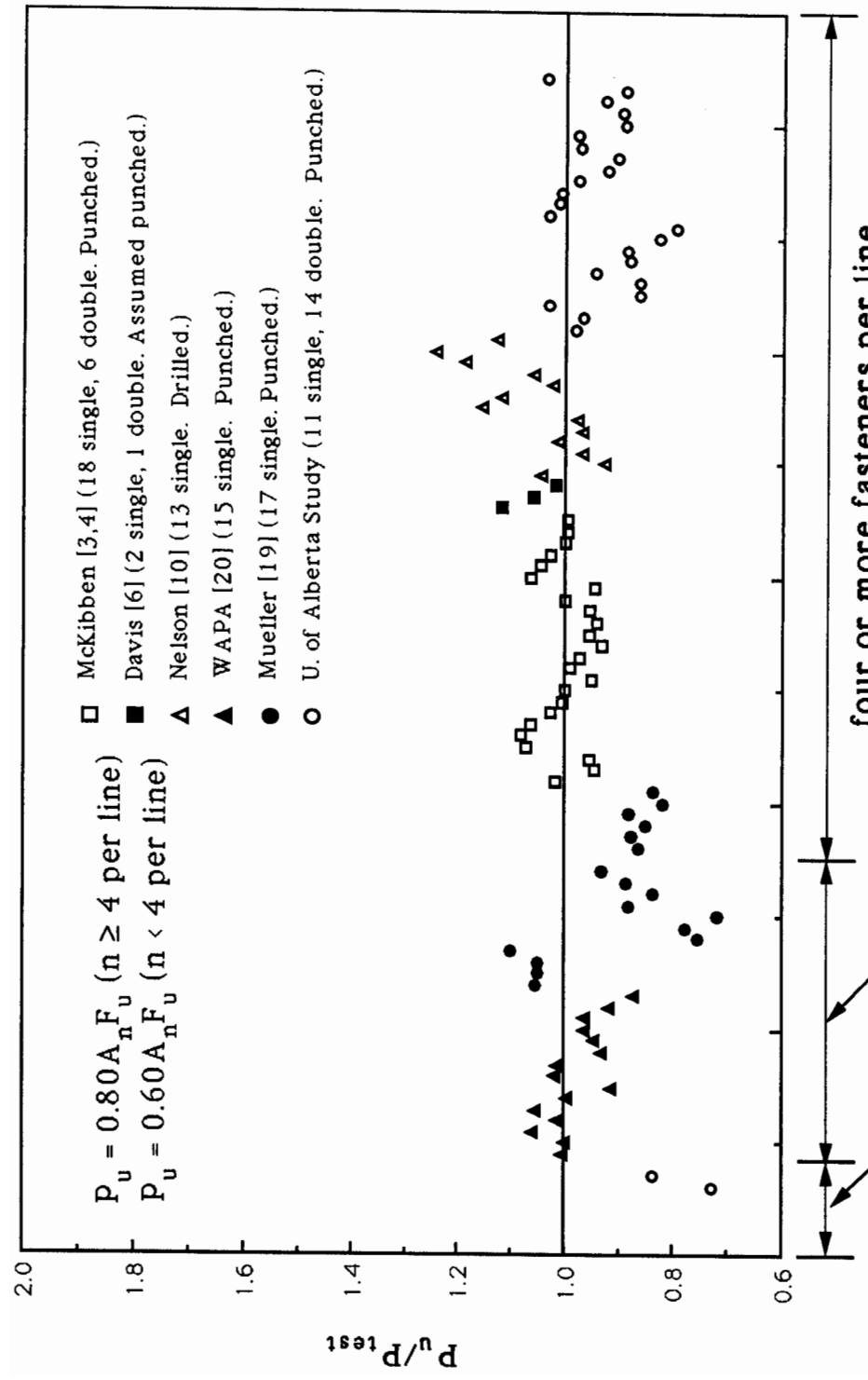

Figure 6.4 Evaluation of Eq. 6.6

7. Summary, Conclusions, and Recommendations

7.1 Summary and Conclusions

This study was undertaken to investigate the effect of shear lag upon the net section strength of single and double angle tension members connected by bolts in one leg. Twenty-four specimens were tested within test parameters that included member length, angle thickness, angle disposition, connection length, and out-of-plane stiffness of the gusset plate for single angles. Finite element analysis was employed subsequently to evaluate the stress distribution at failure at the critical cross-section of the member. The analysis was able to predict the ultimate load of the studied specimens accurately. Based on the study presented herein and together with a critical review of the results obtained by others, the following conclusions can be drawn:

1. The net areas of both single and double angle members in tension are not fully effective if only one leg is connected by fasteners. The net section efficiencies of single and double angles can be treated as practically the same if they are fabricated using the same angle sections and same connection details;
2. The net section efficiency of members with two or three fasteners per line in the connections is significantly lower than for members with four or more fasteners per line in the connections;
3. For an unequal leg angle section, the net section efficiency of the member with the long leg connected is higher than the case with the short leg connected, given that the connection lengths are the same in both cases;
4. The net section efficiency is not affected by either the member length or the angle thickness. The degree of out-of-plane constraint applied to the end of single angles by the gusset plate has little effect on the net section strength;
5. The Munse and Chesson equation (Eq. 6.1), which was presented based on the test results of a large variety of truss-type tension members, has been examined for the particular case of single and double angles. It has been found that this equation is slightly unconservative, provided that the fabrication factor is used together with the shear lag factor. However, the exclusion of the fabrication factor, as is done conventionally, will lead to a significantly unconservative prediction;
6. The AASHTO and AREA design specifications overestimate the net section strength of double angle members. For single angles, the AASHTO and AREA specifications fail to account for the effect of connection length. Consequently, they are conservative for members connected by four or more fasteners per line,

but unconservative if the connection has fewer than four fasteners per line. The ASCE standard is on the unconservative side. The AISC codes and the CAN/CSA-S16.1-M89 standard give an unconservative prediction for both single and double angles. The prediction is especially unconservative in the cases where the connections have fewer than four fasteners per line;

7. It has been shown that Eq. 6.3 accurately predicts the net section strength of single and double angle members. Equations that are more convenient for design purpose (Eq. 6.5 and 6.7) have been developed.

7.2 Recommendations

The factored resistance of bolted single and double angle tension members can be calculated by the following formula:

$$T_r = 0.85\ \text{Ø}\ (F_u\ A_{cn} + \text{ß}\ F_y\ A_o) \qquad [6.5]$$

where T_r = factored resistance of the member

Ø = 0.90

F_u = ultimate strength of the material

F_y = yield strength of the material

A_{cn} = net area of the connected leg at the critical cross-section, computed by taking the diameter of holes 2 mm (1/16 in.) larger than the nominal size

A_o = gross area of the outstanding leg

ß = 1.0 for members with four or more fasteners per line in the connection

= 0.5 for members with fewer than four fasteners per line in the connection

Alternatively, and as a convenience in the design process, the factored resistance of bolted single and double angle tension members can be calculated using the following simplified equations:

$$A_{ne} = U\ A_n \qquad [6.6]$$

and

$$T_r = 0.85\ \text{Ø}\ F_u\ A_{ne} \qquad [6.7]$$

where U = 0.80 if the connection has four or more fasteners per line

= 0.60 if the connection has fewer than four fasteners per line

A_n = net area of the critical cross-section, calculated by taking the hole diameter 2 mm larger than the nominal size

In all the above equations, the punching effect is accounted for by taking the hole diameter 2 mm larger than the nominal size. For a member in which it is known that the holes will be drilled, this requirement may be waived.

References

1. Chesson, E., and Munse, W. H. (1963). "Riveted and bolted joints: truss type tensile connections." *J. of the Struct. Div.*, ASCE, Vol. 89(1), pp 67–106.
2. Munse, W. H., and Chesson, E. (1963). "Riveted and bolted joints: Net section design." *J. of the Struct. Div.*, ASCE, Vol. 89(1), pp 107–126.
3. McKibben, F. P. (1906). "Tension tests of steel angles." *Proc. of the ASTM,* Vol. 6, pp 267–274.
4. McKibben, F. P. (1907). "Tension tests of steel angles with various types of end–connections." *Proc. of the ASTM*, Vol. 7, pp 287–295.
5. Batho, C. (1915). "The effect of the end connections on the distribution of stress in certain tension members." *J. of the Franklin Inst.*, Aug., pp 129-172.
6. Davis, R. P., and Boomsliter, G. P. (1934). "Tensile tests of welded and riveted structural members." *J. of the Amer. Welding Society*, April, pp 21–27.
7. Greiner, J. E. (1897). "Recent tests of bridge members." *Transactions*, ASCE, Vol. 38, pp 41-77.
8. Young, C. R. (1935). *Elementary structural problems in steel and timber.* John Wiley and Sons, New York, N.Y., pp 7.
9. Gibson, G. J., and Wake, B. T. (1942). "An investigation of welded connections for angle tension members." *The Welding J.*, Amer. Welding Society, Vol. 21(1), pp 44s–49s.
10. Nelson, H. M. (1953). "Angles in tension." *Publication No.7*, British Constructional Steelwork Assoc., UK, pp 8–18.
11. Hebrant, F., and Demol, L. (1955). "Tensile tests on riveted connections of rolled sections made of steel A37." *Acier Stahl Steel*, CECM, Vol. 20, pp 178-184.
12. Gaylord, E. H. Jr., Gaylord, C. N., and Stallmeyer, J. E. (1992). *Design of steel structures. (3rd Edition)* McGraw-Hall Inc., New York, N.Y., pp 137-146.
13. Madugula, M. K. S., and Mohan, S. (1988). "Angles in eccentric tension." *J. of the Struct. Eng.*, ASCE, Vol. 114, pp 2387–2396.
14. Amer. Assoc. of State Highway and Transp. Officials (AASHTO). (1983). *Standard specifications for highway bridges.* Washington, D.C.
15. Amer. Inst. of Steel Construction (AISC). (1978). *Specification for the design, fabrication and erection of structural steel for buildings.* Chicago, Ill.
16. Amer. Inst. of Steel Construction (AISC). (1986). *Load and resistance design specification for structural steel buildings.* Chicago, Ill.

17. Canadian Standards Assoc. (CSA). (1984). *CAN3-S16.1-M84, Steel structures for buildings (limit states design).* Rexdale, Ont., Canada.
18. British Standards Inst. (1985). *BS 5950: Part I, Structural use of steel work in building, part 1. Code of practice for design in simple and continuous construction: Hot-rolled sections.* London, UK.
19. Mueller, W. H., and Wagner, A. L. (1985). "Plastic behavior of steel angle columns." *Res. Rept.,* Bonneville Power Admin., Portland, Oreg.
20. Test for Western Area Power Admin. (1987). Private communication received from Prof. M. K. S. Madugula.
21. Canadian Standards Assoc. (CSA). (1989). *CAN/CSA-S16.1-M89, Limit states design of steel structures.* Rexdale, Ont., Canada.
22. Amer. Assoc. of State Highway and Transp. Officials (AASHTO). (1989). *Standard specifications for highway bridges.* Washington, D.C.
23. Amer. Railway Eng. Assoc. (AREA). (1982) *Manual for railway engineering.* Washington, D.C.
24. Amer. Inst. of Steel Construction (AISC). (1989). *Specification for structural steel buildings / Allowable stress design and plastic design.* Chicago, Ill.
25. Amer. Society of Civil Engineers (ASCE). (1991). *Design of latticed steel transmission structures.* New York, N.Y.
26. Amer. Society for Testing and Materials (ASTM). (1992). *A370 Standard test methods and definitions for mechanical testing of steel products.* Philadelphia, PA.
27. Canadian Standards Assoc. (CSA). (1992). *CAN/CSA G40.21-M92, Structural quality steels.* Rexdale, Ont., Canada.
28. Kulak, G. L., Fisher, J. W. and Struik, J. H. A. (1987). *Guide to design criteria for bolted and riveted joints.* John Wiley and Sons, New York, N.Y., pp 99-100.
29. Kohnke, P. C. (1989). *ANSYS engineering analysis system theoretical manual.* Swanson Analysis Systems, Inc., Houston, PA., pp 6.11.1-6.11.4.
30. DeSalvo, G. J., and Gorman, R. W. (1989). *ANSYS engineering analysis system user's manual (Vol. 2).* Swanson Analysis Systems, Inc., Houston, PA., pp 4.43.1-4.43.2.
31. Higgins, T. R. (Dec. 11, 1976). Committee correspondence, AISC Task Committee 9.
32. Canadian Institute of Steel Construction. (1991). *Handbook of Steel Construction. (5th Edition)* Willowdale, Ont., Canada.

Recent Structural Engineering Reports

Department of Civil Engineering

University of Alberta

161. *Analysis of Concrete Panels* by B. Massicotte, A.E. Elwi and J.G. MacGregor, July 1988.

162. *Behavior and Design of Reinforced Concrete Ice-Resisting Walls* by R.M. Ellis and J.G. MacGregor, November 1988.

163. *An Analysis of the Performance of Welded Wide Flange Columns* by D.E. Chernenko and D.J.L. Kennedy, December 1988.

164. *Nonlinear Dynamic Analysis of Caisson-Type Offshore Structures* by I.R. Soudy and T.M. Hrudey, March 1989.

165. *NORCO - A Program for Nonlinear Finite Element Analysis of Reinforced Concrete Structures - Users' Manual* by S. Balakrishnan, A.E. Elwi and D.W. Murray, April 1989.

166. *An Eigenvector Based Strategy for Analysis of Inelastic Structures* by J. Napoleao Fo., A.E. Elwi and D.W. Murray, May 1990.

167. *Elastic Plastic and Creep Analysis of Casings for Thermal Wells* by S.P. Wen and D.W. Murray, May 1990.

168. *Erection Analysis of Cable-Stayed Bridges* by Z. Behin and D.W. Murray, September 1990.

169. *Behavior of Shear Connected Cavity Walls* by P.K. Papinkolas, M. Hatzinikolas and J. Warwaruk, September 1990.

170. *Inelastic Transverse Shear Capacity of Large Fabricated Steel Tubes*, by K.H. Obaia, A.E. Elwi, and G.L. Kulak.

171. *Fatigue of Drill Pipe* by G.Y. Grondin and G.L. Kulak, April 1991.

172. *The Effective Modulus of Elasticity of Concrete in Tension* by Atif F. Shaker and D.J. Laurie Kennedy, April 1991.

173. *Slenderness Effects in Eccentrically Loaded Masonry Walls* by Mohammad A. Muqtadir, J. Warwaruk and M.A. Hatzinikolas, June 1991.

174. *Bond Model For Strength of Slab-Column Joints* by Scott D.B. Alexander and Sidney H. Simmonds, June 1991.

175. *Modelling and Design of Unbraced Reinforced Concrete Frames* by Yehia K. Elezaby and Sidney H. Simmonds, February 1992.

176. *Strength and Stability of Reinforced Concrete Plates Under Combined Inplane and Lateral Loads* by Mashhour G. Ghoneim and James G. MacGregor, February 1992.

177. *A Field Study of Fastener Tension in High-Strength Bolts* by G.L. Kulak and K. H Obaia, April 1992.

178. *Flexural Behaviour of Concrete-Filled Hollow Structural Sections* by Yue Qing Lu and D.J. Laurie Kennedy, April 1992.

179. *Finite Element Analysis of Distributed Discrete Concrete Cracking* by Budan Yao and D.W. Murray, May 1992.

180. *Finite Element Analysis of Composite Ice Resisting Walls* by R.A. Link and A.E. Elwi, June 1992.

181. *Numerical Analysis of Buried Pipelines* by Zhilong Zhou and David W. Murray, January 1993.

182. *Shear Connected Cavity Walls Under Vertical Loads* by A. Goyal, M.A. Hatzinikolas and J. Warwaruk, January 1993.

183. *Frame Methods for Analysis of Two-Way Slabs* by M. Mulenga and S.H.S. Simmonds, January 1993.

184. *Evaluation of Design Procedures for Torsion in Reinforced and Prestressed Concrete* by Mashour G. Ghoneim and J.G. MacGregor, February 1993.

185. *Distortional Buckling of Steel Beams* by Hesham S. Essa and D.J. Laurie Kennedy, April 1993.

186. *Effect of Size on Flexural Behaviour of High Strength Concrete Beams* by N. Alca and J.G. MacGregor, May 1993.

187. *Shear Lag in Bolted Single and Double Angle Tension Members* by Yue Wu and Geoffrey L. Kulak, June 1993.